Institut für Veterinärbakteriologie
Abteilung für Geflügel- und Kaninchenkrankheiten
der Vetsuisse-Fakultät Universität Zürich

Direktor *ad interim*: Prof. Dr. Dr. h.c. Roger Stephan

Arbeit unter wissenschaftlicher Betreuung von
Dr. Nina Wolfrum

Generation of an Infectious Laryngotracheitis Reporter Virus

Inaugural-Dissertation

zur Erlangung der Doktorwürde der
Vetsuisse-Fakultät Universität Zürich

vorgelegt von

Simone Martina Meier

Tierärztin
von Bachenbülach, ZH

genehmigt auf Antrag von

Prof. Dr. med. vet. Richard K. Hoop, Referent
Prof. Dr. sc. nat. Cornel Fraefel, Korreferent

2017

Institut für Veterinärbakteriologie
Abteilung für Geflügel- und Kaninchenkrankheiten
der Vetsuisse-Fakultät Universität Zürich

Direktor *ad interim*: Prof. Dr. Dr. h.c. Roger Stephan

Arbeit unter wissenschaftlicher Betreuung von
Dr. Nina Wolfrum

Generation of an Infectious Laryngotracheitis Reporter Virus

Inaugural-Dissertation

zur Erlangung der Doktorwürde der
Vetsuisse-Fakultät Universität Zürich

vorgelegt von

Simone Martina Meier

Tierärztin
von Bachenbülach, ZH

genehmigt auf Antrag von

Prof. Dr. med. vet. Richard K. Hoop, Referent
Prof. Dr. sc. nat. Cornel Fraefel, Korreferent

2017

to my nearest and dearest

Table of Contents

1. Summary

1.1 Summary

The understanding of pathogen host interactions is crucial for the development of vaccines and therapeutics against infectious diseases. Prerequisites for studying such interactions are appropriate techniques and tools. For example, monitoring a virus` life cycle is possible with several microscopy techniques. But since viruses are to small to be seen with most of the existing microscopes, they have to be modified. A commonly used technique is labelling of the virus with a fluorescent dye or protein. Such reporter-viruses can be generated by a chemical modification or by a genetic alteration of the virus genome.

This work aimed at the generation of an infectious laryngotracheitis (ILT) reporter virus, that will enable a real time monitoring of host cell infections. For this purpose, protein fragments of ILTV were fused to a fluorescent protein (mNeonGreen; mNG). Furthermore, cell lines were generated that stably express this fusion protein and provide it *in trans* to facilitate the incorporation into newly build ILT particles.

This reporter virus should enable new insights into the infection pathway of ILTV and thus will be important for combating the epizootic disease which causes immense economic losses in poultry production worldwide.

Keywords: Infectious laryngotracheitis virus, GaHV-1, reporter virus, mNeonGreen, stable cell line

1.2 Zusammenfassung

Eine Voraussetzung zur Entwicklung von Impfungen und Therapien gegen Infektionskrankheiten ist das grundlegende Verständnis der Pathogen-Wirt-Interaktionen. Zum Studium dieser Interaktionen sind geeignete Methoden und Werkzeuge erforderlich. Durch verschiedene Mikroskopie-Techniken lassen sich z.B. virale Infektionswege verfolgen. Viren sind jedoch zu klein, um für die meisten bildgebenden Verfahren sichtbar zu sein. Daher müssen sie modifiziert werden. Eine gängige Methode ist die Markierung mittels fluoreszierendem Farbstoff oder Protein. Solche Reporter-Viren können durch chemische oder genetische Modifikation des Virusgenoms erzeugt werden.

Die hier vorgestellte Arbeit hatte das Ziel, ein Reporter-Virus, basierend auf dem Infektiösen Laryngotracheitis (ILT) Virus, herzustellen, welches die Echtzeit-Beobachtung der Infektion von Zellen ermöglichen soll. Dazu wurden Fragmente eines ILTV Proteins mit einem fluoreszierenden Protein (mNeonGreen; mNG) fusioniert. Des Weiteren wurden Zelllinien generiert, welche diese Fusionsproteine stabil exprimieren und dadurch *in trans* zur Verfügung stellen, um deren Inkorporation in neugebildete ILT Partikel zu ermöglichen.

Dieses Reporter-Virus soll neue Einblicke in den Infektionszyklus von ILTV liefern und ist daher wichtig für die Bekämpfung der Tierseuche, die weltweit immense ökonomische Verluste in der Geflügelproduktion verursacht.

Stichworte: Infektiöses Laryngotracheitis Virus, GaHV-1, reporter virus, mNeonGreen, stabile Zelllinie

2. Introduction

Infectious laryngotracheitis caused by the homonymous virus, also known as Gallid alphaherpesvirus 1, is a worldwide occurring, highly contagious, respiratory disease with a narrow host range. Susceptible species are chicken, pheasants and peafowls [1]. Infected animals show symptoms ranging from conjunctivitis and serous nasal discharge to haemorrhagic tracheitis with dyspnoea and expectoration of sanguineous mucus [2], [3]. In severe cases, 5% to 72% of infected animals will die [4]. But even without severe symptoms, ILTV infection leads to reduced weight gain and decreased egg production which has a huge economic impact [5]. Animals surviving the acute phase lasting for 1 to 2 weeks [4], still harbour the virus in a latent state, mainly in the trigeminal ganglion [6]. Immunosuppressive and stressful circumstances can lead to a reactivation of the virus and thus shedding of infectious particles [7], which can be a threat for other susceptible birds.

Today the clinical manifestation of ILT is well known. Furthermore, the virus life cycle is characterized on the level of target organs and tissues. Virus replication primary takes place in the tracheal tissue, however, other mucus membranes like conjunctiva, respiratory sinuses, air sacs and the lung can be infected as well [5], [8]. Even though a lot is known about the basic biology of ILTV, a detailed understanding of the cellular mechanisms during infection, like cell entry, replication and egress of ILTV, is not yet entirely revealed. A more precise picture of ILTV-host interactions could help to improve intervention strategies.

Currently no specific treatment against ILT is possible. For controlling the disease, various vaccines are available and are applied in several countries worldwide. One drawback of these vaccines is the challenge to differentiate between field isolates and vaccination strains, which is not possible with routine diagnostic methods. Furthermore, the commonly used live attenuated virus vaccines bear the risk of reversion and recombination with field strains due to latency [9], [10], [11].

The development of safe DIVA-vaccines (Differentiating Infected from Vaccinated Animals) is in high demand, since the serious and significant effects of ILT in animal welfare and economics. To achieve this, it is crucial to understand the virus' interaction with its host cells. To gain further insights, reporter viruses have been shown to operate as a useful tool to visualize various events of the viral life cycle [12], [13]. Fluorescently labelled viruses even allow for real time monitoring of certain infection steps and may help to understand those mechanisms in more detail.

2.1 Infectious Laryngotracheitis Virus

2.1.1 Taxonomy

ILTV belongs to the family *Herpesviridae*, subfamily *Alphaherpesvirinae* [14], [15]. Alphaherpesviruses are divided into six genera. GaHV-1 and the Psittacid alphaherpesvirus 1 (PsHV-1), the causative pathogen of Pacheco's disease in psittacine birds, are the only two members assigned to the genus *Iltovirus* (Fig. 1). Iltoviruses represent a phylogenetically unique class of alphaherpesviruses analysed by comparison of nucleotide sequence, gene content and genomic organization [14], [16]. ILTV exhibits a considerable evolutionary distance from most other avian and mammalian alphaherpesviruses [14], [16], [17].

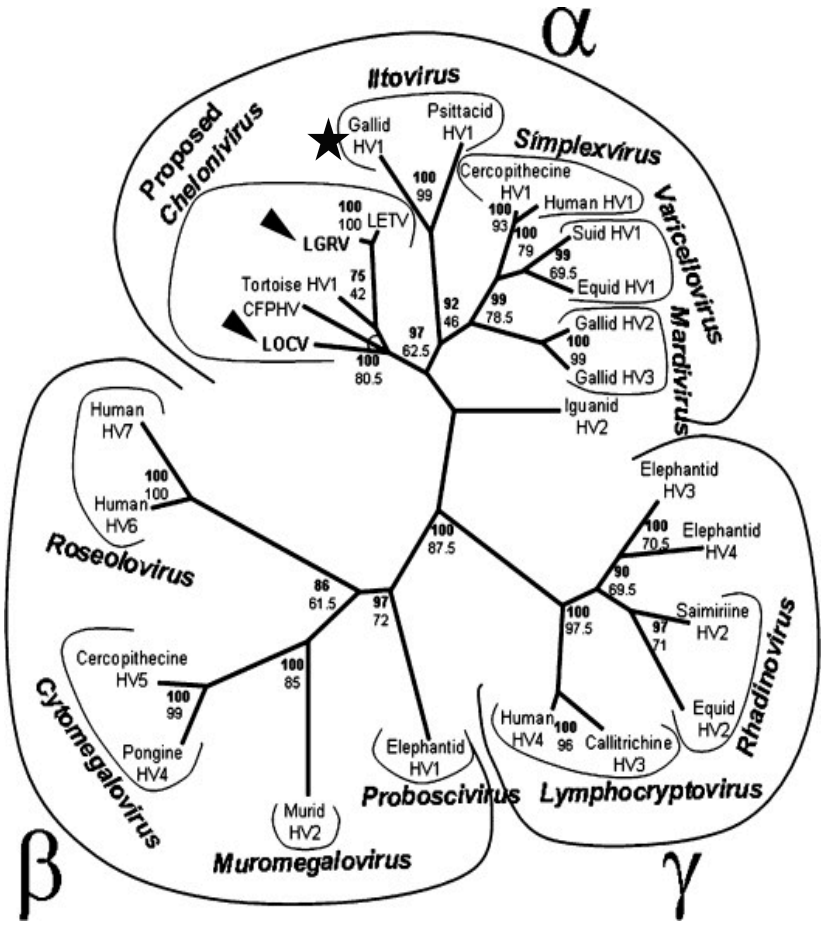

FIG. 1. Phylogenetic tree of *Herpesviridae.* Stacy et al., VetMicrobiol., 2008
Demonstration of considerable distance of GaHV-1 (marked with a star) to other avian and mammalian herpesviruses apart from PsHV-1 which is also assigned to the genus *Iltovirus* within the subfamily *Alphaherpesvirinae.*

2.1.2 Morphology and genome organization

The ILTV genome consists of a linear double-stranded DNA molecule [5], 148,665 base pairs (bp) in length [14]. The icosahedral nucleocapsid measures 80 – 100 nm in diameter and is surrounded by various tegument proteins. The irregular envelope is spiked with characteristic glycoproteins and measures 195 – 250 nm in diameter (Fig. 2) [5].

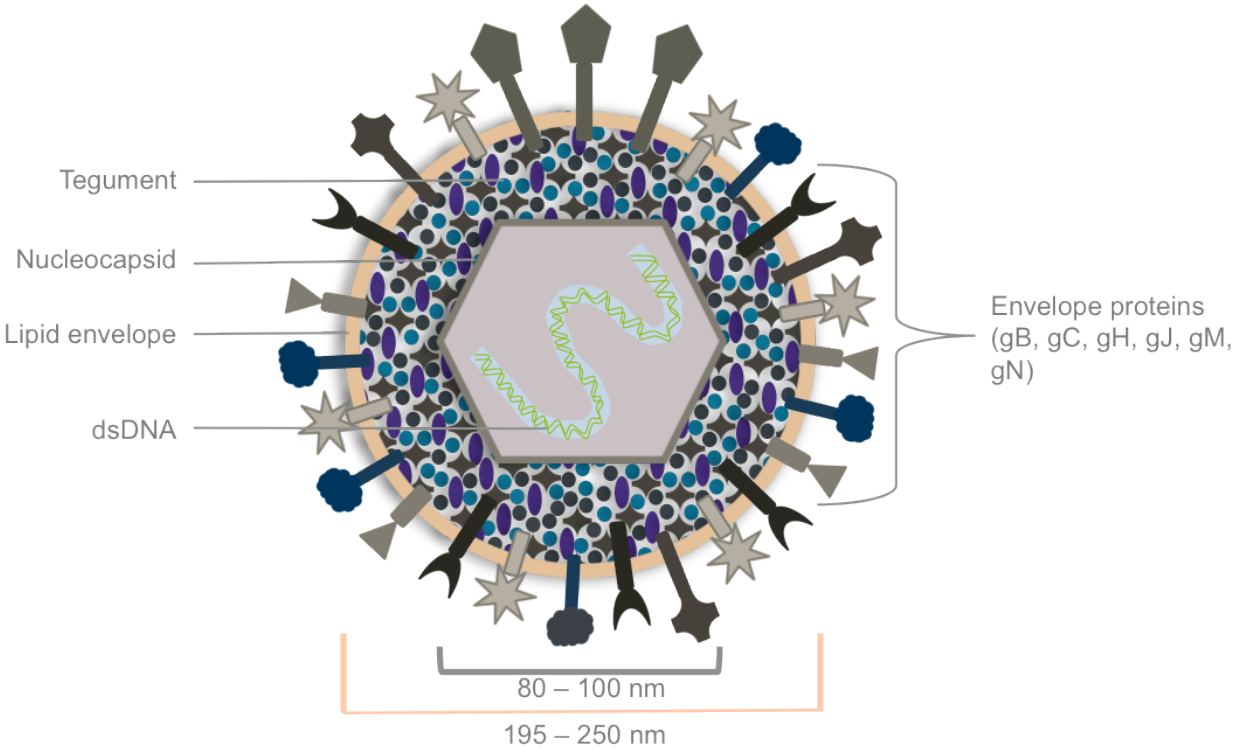

FIG. 2. Scheme of ILTV morphology.
The linear double stranded DNA is located in the icosahedral nucleocapsid, which is itself wrapped in a proteinaceous layer (tegument) and a lipid bilayer called envelope. The envelope is spiked with various glycoproteins. The whole viral particle measures 195 to 250 nm in diameter.

Most of the designations for open reading frames (ORFs) and proteins of ILTV were adopted from the homologues in herpes simplex virus type 1 (HSV-1) [18], [19]. The ILTV genome compromises two domains of unique sequences, the unique short (US) region and the unique long (UL) region. Only the US region is flanked by internal repeats and terminal repeats, respectively [14], [20], allowing the existence of two isomeric forms with an inversion of the US region only [21]. This specific genome structure classifies the ILTV genome as a class D herpesvirus genome [14]. Altogether 77 ORFs were predicted along the ILTV genome [14]. The UL region contains 62 genes and includes a block of five unique, conserved ORFs (A to E, Fig. 3, marked with circles) [14]. An additional characteristic for ILTV's UL region is an inversion from UL22 to UL44 (Fig. 3, marked with stars) [14], [22], [23]. No homologue of UL16 could be found in the ILTV genome. The US region contains 9 genes and is flanked by

the inverted repeat regions containing two copies of the genes: ICP4, US10 and SORF4/3 (Fig. 3, marked with triangles). Five structural glycoproteins were predicted to be encoded by the US region [14].

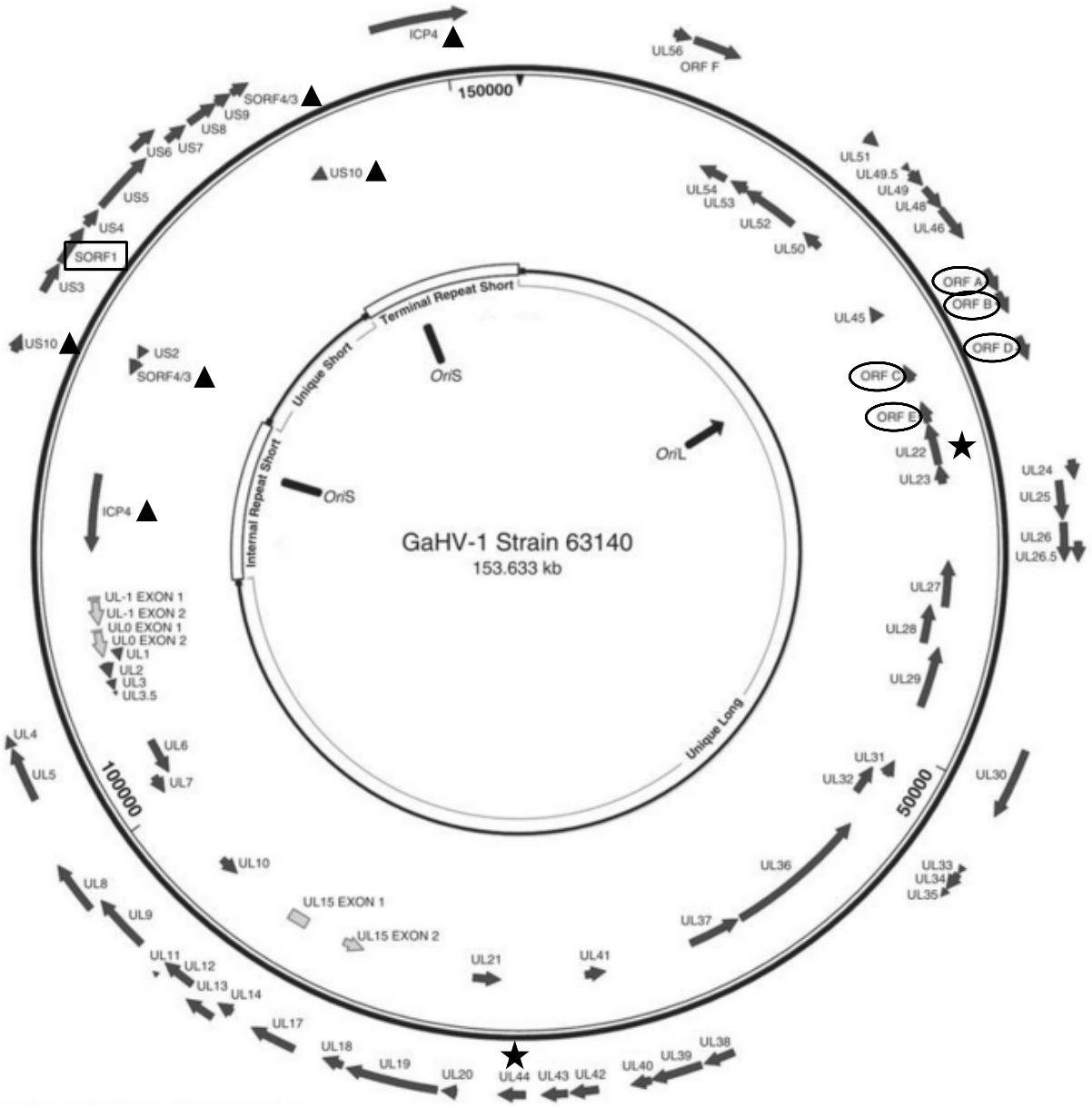

FIG. 3. Scheme of GaHV-1 genome content [5].
The five conserved, unique ORFs are marked with circles. The three genes in copy within the inverted repeats are marked with triangles. The stars indicate the inversion of the genome region from UL22 to UL44. The rectangle marks the SORF1 gene, encoding the abundant tegument phosphoprotein UL47.

2.1.3 ILTV UL47

In comparison with most alphaherpesviruses, the UL47 gene (also SORF1) of ILTV and PsHV-1 is translocated from the UL region to the US region (Fig. 3, marked with a rectangle). It is located between the conserved genes US3 (protein kinase) and US4 (glycoprotein G) [14], [22], [24], [25]. The ILTV UL47 gene encodes for an abundant tegument phosphoprotein [24]. The role of UL47 during infection is not yet investigated properly. In HSV-1, pseudorabies virus (PrV) and Marek's disease virus serotype 1 (MDV-1, renamed to gallid alphaherpesvirus 2), UL47 seems to be non-essential for replication *in vitro* [26], [27], [28]. Nevertheless, adverse effects were observed: reduced plaque sizes formed by PrV- and MDV-1-ΔUL47 viruses [26], [27], smaller and less electron-dense tegument surrounding the capsids produced by PrV-ΔUL47 mutants [27], and severe growth impairment in MDV-1 strains with a deletion of the UL47 gene [26]. Furthermore, deletion of the UL47 gene in PrV led to an impairment of the secondary envelopment with subsequent accumulation of tegumented capsids within the cytoplasm [27]. Beyond that, it led to a moderate attenuation in experimentally infected mice in correlation with a slower neuroinvasion rate and influence on neurovirulence [29].

Aiming at the development of safer vaccines against ILTV, construction of virus mutants bearing a deletion of a particular gene could be a conceivable approach. In case of UL47, Helferich et al. investigated the growth properties of ILTV mutants lacking the UL47 gene *in vitro* and the relevance for virulence and immunogenicity *in vivo* [24]. Similar to PrV and MDV-1, they could reveal that ILTV UL47 is not essential for *in vitro* replication. Furthermore, plaque size was reduced by 95% compared to wild type ILTV and maximum titre was around 10-fold lower. Chickens infected with the UL47-deletion mutant developed only moderate respiratory symptoms and recovered completely. Additionally, Helferich et al. ruled out that UL47 is relevant for the humoral immune response. Hence, possible protection potential of a mutant lacking the UL47 gene was investigated. Challenge experiments resulted in the absence of marked clinical symptoms and no lesions within the trachea were found by histopathology. Moreover, no ILT virus could be re-isolated. Nevertheless, in tracheal swabs ILTV DNA was detectable by PCR.

2.1.4 Virion packaging signal (VPS)

In a study of Schlegel and Blaho 2009 [30], an incidentally generated in-frame fusion of the green fluorescent protein (GFP) to the carboxy-terminal end of the abundant tegument protein VP22 occurred and resulted in the packaging of GFP into HSV-1 particles. GFP alone was not incorporated into virions. This let to the hypothesis of the existence of a virion packaging signal at the C-terminal end of VP22. Finally, they identified a domain within the last 15 amino acids of VP22, which contains a motif of six consecutive amino acids: ARSASR. This sequence is conserved among HSV-1, herpes simplex virus type 2 (HSV-2) and varicella zoster virus (VZV).

The alignment of HSV-1 VP22 with various ILTV sequences revealed a similar amino acid motif at the carboxy-terminal end of UL47 (Fig. 4. ARSASR in HSV-1 and AVSARR in ILTV). This let us to the assumption that this domain might be responsible for packaging of UL47 into ILTV particles. Besides this similarity within the C-terminal sequence, no major sequence homologies are apparent. Furthermore, it should be noted that ILTV UL47 consists of 623 amino acids in total compared to 301 amino acids for HSV-1 VP22 (deduced from GenBank DNA sequences NC_006623 and NC_001806).

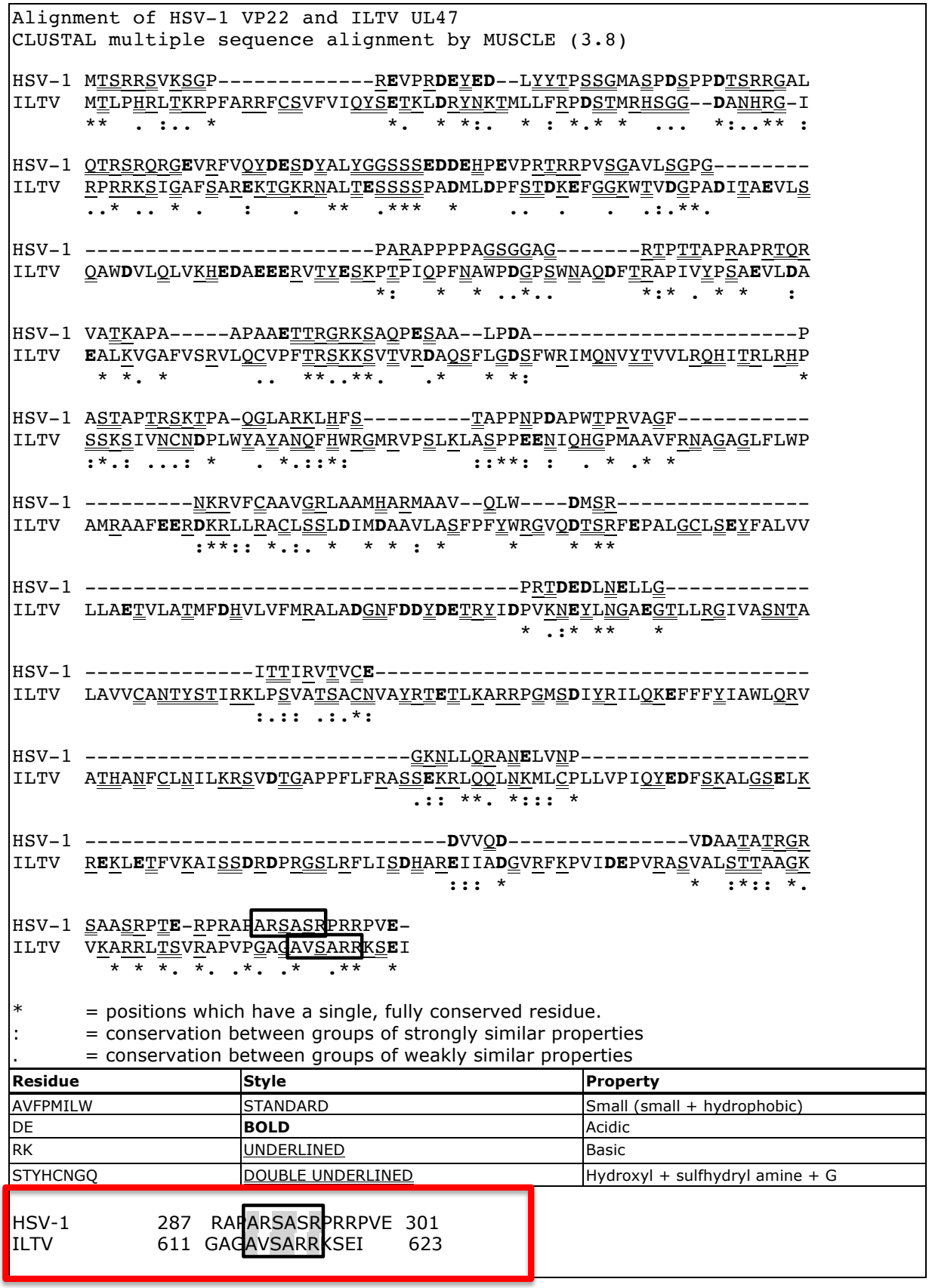

FIG. 4. Alignment of HSV-1 VP22 and ILTV UL47.
The rectangle marks the similar consecutive motif of six amino acids at the C-terminal end, ARSASR in HSV-1 or AVSARR in ILTV respectively. Identical amino acids are highlighted in grey.

2.2 Reporter virus

Reporter viruses are widely used in research. Basically two types of reporter viruses are distinguished:

- Viruses, which express a marker gene such as GFP or luciferase. Therefor the marker gene needs to be incorporated into the viral genome and thus will be expressed in infected cells. By measuring the resulting fluorescence or luminescence respectively, quantitative information about the infection can be obtained.

- Viruses, which are tagged by fluorescent dyes (e.g. Cyanine or Phycoerythrin; Cy3, PE) or by one or more marker proteins (e.g. green or red fluorescent protein; GFP, RFP). The marker proteins are modified in a way that they get incorporated into viral particles. This allows monitoring of individual viruses and real-time tracking of ongoing infection steps like cell binding and virus entry.

The few things known about the replication cycle of ILTV were mainly adapted from the knowledge about other alphaherpesviruses. To provide a tool for further investigations of ILTV-cell-interactions, the development of a reporter virus incorporating a fluorescent protein is useful and demanded. Aiming at a more detailed understanding of early steps of infection (virus attachment and entry), the second type of reporter virus was chosen in the herein presented work.

2.3 The monomeric green fluorescent protein

The monomeric variant of the Neon Green protein (mNG) is derived from *Branchiostoma lanceolatum*, a lancelet belonging to the order *Amphioxiformes*, subphylum *Cephalochordata*. Compared with most commonly used green and yellow fluorescent proteins, it has superior optical properties with a high quantum yield and extinction coefficient, resulting in the brightest monomeric green or yellow fluorescent protein yet described [31]. The performance of mNG as fluorescent probe in live-cell imaging has been successfully determined, what gives us the reason to choose mNG as fluorescent marker in our investigations. The pNCS-mNeonGreen plasmid delivers mNG for our study (Fig. 9, mNG is marked with a star).

2.4 Stable cell lines generated with retroviral vectors

Stable cell lines were established by transduction with retroviral vectors. Those were generated by transfecting producer cells with three plasmids: the packaging construct (pHit60), the envelope construct (pMD2.G) and the respective transfer vectors including the long terminal repeats (LTR's) and the packaging signal ψ (Fig. 5). The retroviral vectors were used for transduction of leghorn male hepatoma cells (LMH) to achieve a stable insertion of the transfer vectors into the cellular genome. LMH cells are supposed to be the only permanent cell line, which enables replication of ILTV [32], [33], [34]. Subsequent selection for cells with inserted transfer vectors was achieved by antibiotic selection, since an antibiotic resistance gene was also delivered by the transfer vector (Fig. 10, marked with a star).

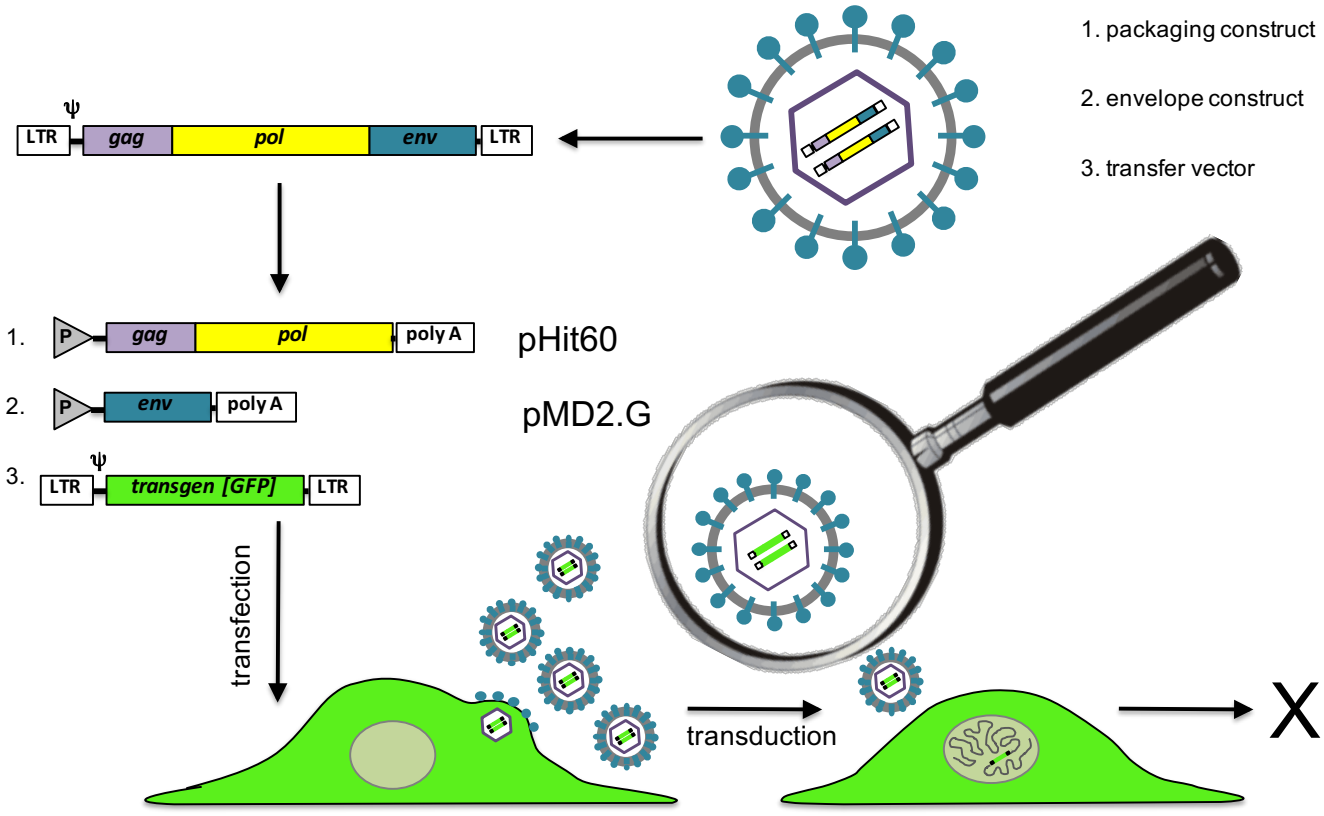

FIG. 5. Schematic illustration of transfection and transduction experiments to obtain stable cell lines.
Three plasmids were used to transfect suitable cell lines: packaging constructs pHit60, envelope constructs pMD2.G and the respective transfer vectors. Selection of cell lines was done by adding antibiotics, marked with "X".

2.5 Aim of the study

This project is focused on the generation of an ILT reporter virus with incorporated mNeonGreen-UL47 fusion protein, enabling live monitoring of ILTV *in vitro*. The tegument proteins are incorporated into virus particles due to a specific virion packaging signal (VPS). For HSV-1 VP22, this sequence was identified as six amino acids (ARSASR) at the C-terminal domain. It is conserved among HSV-1, HSV-2, and VZV [30]. For ILTV UL47, such a sequence is not known yet. HSV-1 VP22 and ILTV UL47 only share 28.5% sequence homology. Furthermore, ILTV UL47 is about twice as big as HSV-1 VP22. Nevertheless, the carboxy-terminus of ILTV UL47 contains an amino acid sequence (AVSARR) pretty close to the identified packaging signal for HSV-1 (Fig. 4).

To identify the ILTV UL47 VPS, different overlapping fragments of the UL47 gene were fused to the monomeric neon green protein (mNG). First, transient expression of the newly generated constructs was tested in LMH cells. Thereupon, stable cell lines were generated by transduction with retroviral transfer vectors and subsequent selection of the cells. The stable cell lines were used to produce an ILTV mutant virus that lacks the wild type (wt) UL47 protein. It was supposed to incorporate the mNG fused to the putative VPS (Fig. 6).

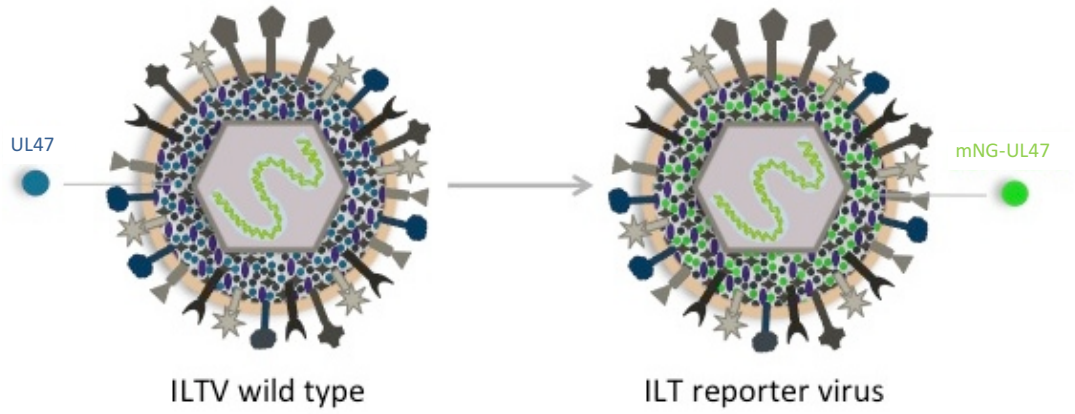

FIG. 6. Model of ILT reporter virus with incorporated mNG-UL47 fusion proteins.
In wild type ILTV, UL47 is an abundant tegument protein. When fused to mNG, this should also be widely distributed among the tegument.

3. Material and Methods

3.1 Material

3.1.1 Chemical reagents

Reagent	Origin	
Cloning experiments		
1 Kb Plus DNA Ladder	Thermo Fisher Scientific	
	www.thermofisher.com	Cat. No. 10787-018
5x Fusion HF Buffer	Thermo Fisher Scientific	
	www.thermofisher.com	Cat. No. F518L
10x DNA loading buffer	1.5 g Ficoll 400, 2 ml EDTA, 0.5 ml bromophenol blue, ad 7 ml H_2O	
Adenosine triphosphate (dATP)	Thermo Fisher Scientific	
	www.thermofisher.com	Cat. No. R0141
Agarose, LE, Analytical Grade	Promega Corporation / Promega AG, Dübendorf CH	
	www.promega.com	Cat. No. V3125
Buffer O	Thermo Fisher Scientific - France, Illkirch FR	
	www.thermofisher.com	Cat. No. BO5
dNTPs	QIAGEN AG, Hombrechtikon CH	
	https://www.qiagen.com	Cat. No. 201900
Double-distilled water (ddH_2O)	Prepared in laboratory at institute of veterinary bacteriology	
	University of Zurich, Switzerland	
Ethidium bromide solution (EtBr) 1%	Carl Roth GmbH + Co. KG / Roth AG, Arlesheim CH	
	www.carlroth.com / www.carlroth.ch	Cat. No. 2218.1
LB-agar plates (incl. 100 µg/ ml Ampicillin) Difco TM	Becton Dickinson AG, Allschwil CH	
	www.bdbiosciences.com	Cat. No. 244520
LB-Amp medium	5 ml LB broth, 5 µl Ampicillin	
LB Broth	Becton Dickinson AG, Allschwil CH	
	www.bdbiosciences.com	Cat. No. 244620
NEBuffer 3.1	New England Biolabs / Bioconcept, Allschwil CH	
	www.neb.com / www.bioconcept.ch	Cat. No. B7203S
S.O.C. Medium	Thermo Fisher Scientific	
	www.thermofisher.com	Cat. No. 15544-034
TAE Buffer	0.4 M Tris, 0.1 M Na_2EDTA pH 8.0, 0.2 M glacial acetic acid	
Transfection		
DMEM	Dulbecco's Modified Eagle Medium	Sigma Aldrich Chemie GmbH, Buchs CH
		www.sigmaaldrich.com Cat. No. D6429
FBS	Fetal Bovine Serum 10%	Thermo Fisher Scientific
		www.thermofisher.com Cat. No. 10270106
Opti-MEM®	Reduced Serum Medium, no phenol red	Thermo Fisher Scientific
		www.thermofisher.com Cat. No. 11058021

Penicillin-Streptomycin	Antibiotic agent	Thermo Fisher Scientific	
		www.thermofisher.com	Cat. No. 15140148
*Trans*IT®-2020	Transfection reagent	Mirus Bio LLC / LabForce AG, Muttenz CH	
		https://www.mirusbio.com	Cat. No. MIR 5400
Trypan Blue solution	Staining, detection of damaged/dead cells	Sigma Aldrich Chemie GmbH, Buchs CH	
		www.sigmaaldrich.com	Cat. No. T8154
Trypsin-EDTA solution	Adherent cells separation	Sigma Aldrich Chemie GmbH, Buchs CH	
		www.sigmaaldrich.com	Cat. No. T3924

Transduction

Dulbecco's phosphate buffered saline (PBS)	Balanced salt solution	Sigma Aldrich Chemie GmbH, Buchs CH	
		www.sigmaaldrich.com	Cat. No. D8537
G418	Aminoglycoside AB (Geneticin-Disulphate)	Carl Roth GmbH + Co. KG / Roth AG, Arlesheim CH	
		www.carlroth.com / www.carlroth.ch	Cat. No. CP11.2
Paraformaldehyde	Cell fixation	Carl Roth GmbH + Co. KG / Roth AG, Arlesheim CH	
		www.carlroth.com / www.carlroth.ch	Cat. No. 0335.1
Polybrene	Cationic polymer	Sigma Aldrich Chemie GmbH, Buchs CH	
		www.sigmaaldrich.com	Cat. No. 107689
Waymouth's medium	Cell culture medium	Thermo Fisher Scientific	
		www.thermofisher.com	Cat. No. 31220-023

Western blot

6x Loading buffer (Lämmli)	5 ml glycerine 87%, 2.5 ml β-mercaptoethanol, 15 ml sodium dodecyl sulphate 10%, 6.25 ml upper Tris, 12.5 mg bromphenol blue, ad 50 ml H_2O	
BenchMark™ Pre-Stained Protein Ladder	Thermo Fisher Scientific	
	www.thermofisher.com	Cat. No. 10748010
Blocking buffer	5% non-fat dry milk powder in TBS 1x	
Blotting buffer	100 ml chamber buffer, 150 ml methanol, ad 1000 ml H_2O	
Chamber buffer 10x	30.275 g Tris-hydroxy-methyl-aminomethan, 144.134 g glycine, ad 1000 ml H_2O	
Enhanced chemiluminescence (ECL) reagent	1 ml Solution A, 0.3 µl H_2O_2 35%, 100 µl Solution B Solution A: 500 ml 0.1 M Tris-HCl (pH 8.6), 125 mg Luminol Solution B: 11 mg para-hydroxycoumarin acid, 10 ml dimethyl sulfoxide	
Lower Tris	91 g Tris, 400 ml H_2O, HCl until pH 8.8, 20 ml SDS 10%, ad 250 ml H_2O	
Separation gel (10%)	10 ml H_2O, 8.4 ml 30% acrylamide/Bis solution, 6.5 ml lower Tris pH 8.8, 15 µl tetramethylenethylendiamine, 200 µl ammonium persulfate 10%	
Stacking gel	6.5 ml H_2O, 1 ml 30% acrylamide/Bis solution, 2.5 ml upper Tris pH 6.8, 20 µl tetramethylenethylendiamine, 40 µl ammonium persulfate 10%	
Rapilait, non-fat dry milk powder	Migros, LeShop	
	www.leshop.ch	EAN 7610200017598
RIPA Lysis Buffer	Santa Cruz Biotechnology, Heidelberg DE	
	www.scbt.com	Cat. No. sc-14948

TBS	19.8 mM Tris, 500 mM NaCl	
TTBS	TBS 1x, 0.05% Tween 20	
Upper Tris	15.25 g Tris, 400 ml H_2O, HCl until pH 6.8, 10 ml SDS 10%, ad 250 ml H_2O	
Infection experiment		
Goat serum	Thermo Fisher Scientific	
	www.thermofisher.com	Cat. No. 16210064
Poly-L-lysine solution	Sigma-Aldrich Chemie GmbH, Buchs CH	
	www.sigmaaldrich.com	Cat. No. A-005-C

TABLE 1. Chemical reagents and their origin.
Chemical reagents used for cloning of mNG-UL47 fusion fragments, transfection of 293T cells, transduction of LMH cells, Western blot analysis of UL47 fusion proteins as well as infection of LMH cells and generation of ILT reporter viruses.

3.1.2 Enzymes and buffers

Enzyme	**Buffer**	**Origin**	
Restriction Enzymes			
BamHI	NEBuffer 3.1	New England Biolabs / Bioconcept, Allschwil CH	
		www.neb.com / www.bioconcept.ch	Cat. No. R0136S
BglII	NEBuffer 3.1	New England Biolabs / Bioconcept, Allschwil CH	
		www.neb.com / www.bioconcept.ch	Cat. No. R0144S
Eco47III (AfeI)	Buffer O	Thermo Fisher Scientific - France, Illkirch FR	
		www.thermofisher.com	Cat. No. ER0321
NotI	NEBuffer 3.1	New England Biolabs / Bioconcept, Allschwil CH	
		www.neb.com / www.bioconcept.ch	Cat. No. R0189S
DNA Polymerase			
Phusion HighFidelity DNA Polymerase	Phusion HF	Thermo Fisher Scientific - France, Illkirch FR	
		www.thermofisher.com	Cat. No. F530S
Ligase			
T4 DNA Ligase	NEBuffer 3.1	New England Biolabs / Bioconcept, Allschwil CH	
		www.neb.com / www.bioconcept.ch	Cat. No. M0202S

TABLE 2. Enzymes and buffers and their origin.
Enzymes and buffers used for cloning of mNG-UL47 fusion fragments.

3.1.3 Plasmids and DNA

Plasmid, DNA	Features	Origin	
Cloning experiments			
ILTV DNA	Isolated from the virulent A-489 ILTV strain	Federal Research Institute for Animal Health', Friedrich-Loeffler-Institut, Greifswald-Insel Riems, Germany	
pLEGFP-N1	Retroviral vector	Becton Dickinson AG, Allschwil CH	
		www.bdbiosciences.com	Cat. No. 6059-1
pNCS-mNeonGreen (pNCS-mNG)	Bacterial expression vector. Constitutively expressing 6xHis-tagged mNeonGreen in *E. coli*	Allele Biotechnology, San Diego, CA, USA	
		www.allelebiotech.com	Cat. No. ABP-FP-MNEONSB
Transfection			
pHit60	packaging construct, derived from murine leukemia virus, encoding for gag and pol	Soneoka et al., 1995 [35]	
pMD2.G	envelope construct, derived from Vesicular Stomatitis Virus	A gift from Didier Trono (unpublished)	
pL-mNG-N1	Transfer vector	In the presented work	

TABLE 3. Plasmids and DNA and their origin.
Plasmids an DNA used for cloning of mNG-UL47 fusion fragments and for transfection of 293T cells.

3.1.4 Primers

Origin: Microsynth AG, Balgach CH
www.microsynth.ch

Name	Nucleotide sequence	Length
BglII_*mNG*(+)	GTACTAGATCTCCACC***ATG***GTGAGCAAGGGCGAGGAGGATAAC	43mer
mNG(-)	ACTACCACCACCACC*CTTGTACAGCTCGTCCATGCCCATCAC*	42mer
*mNG*_Not(-)	GGAAGCGGCCGCTCC**TCA***CTTGTACAGCTCGTCCATGCCCATCAC*	45mer
1UL47_1-75(+)	GGTGGTGGTGGTAGTACCTTGCCCCATCGATTAACGAAAAG	41mer
1UL47_1-75_Not(-)	GGAAGCGGCCGCTCCTCATTTTCCAGTCTTTTCGCGCGCGCTAAAC	46mer
2UL47_60-155(+)	GGTGGTGGTGGTAGTAGGCGGAAATCTATTGGAGCGTTTAGC	42mer
2UL47_60-155_Not(-)	GGAAGCGGCCGCTCC**TCA**ACTCGGCCCGTCCGGCCAGGCATTGAAC	46mer
3UL47_140-245(+)	GGTGGTGGTGGTAGTAAACCGACCCCGATACAGCCGTTCAATG	43mer
3UL47_140-245_Not(-)	GGAAGCGGCCGCTCC**TCA**GTTGCAGTTAACAATGCTTTTGCTGG	44mer
4UL47_230-335(+)	GGTGGTGGTGGTAGTATAACTCGACTCAGGCACCCTTCCAGC	42mer
4UL47_230-335_Not(-)	GGAAGCGGCCGCTCC**TCA**GACGCCGCGCCAGTAAAATGGAAACGAC	46mer
5UL47_321-430(+)	GGTGGTGGTGGTAGTGACGCAGCCGTCCTCGCGTCGTTTCCA	42mer
5UL47_321-430_Not(-)	GGAAGCGGCCGCTCC**TCA**TTTTCTTATCGTCGAATAGGTGTTTGC	45mer
6UL47_380-470(+)	GGTGGTGGTGGTAGTGGCAATTTCGATGACTATGACGAAACTAG	46mer
6UL47_380-470_Not(-)	GGAAGCGGCCGCTCC**TCA**AATGTAAAAGAAAAACTCTTTTTGTAA	45mer
7UL47_456-555(+)	GGTGGTGGTGGTAGTAGCGACATATACCGGATATTACAAAAAGAG	45mer
7UL47_456-555_Not(-)	GGAAGCGGCCGCTCC**TCA**CCCCCTCGGGTCCCTGTCGCTGGAAATAG	47mer
8UL47_540-622(+)	GGTGGTGGTGGTAGTTTAGAGACATTCGTTAAAGCTATTTCC	42mer
8UL47_540-622_Not(-)	GGAAGCGGCCGCTCC**TCA**TATTTCCGATTTCCGGCGCGCGGAAAC	46mer
9BglII_*mNG*(+)	GTACTAGATCTCCACC***ATG***GTGAGCAAGGGCGAGGAGGATAACATGGCCTCTCTCCCAGCGACACATGAGTTA	73mer
9UL47_610-622_Not(-)	GGAAGCGGCCGC**TCA**TATTTCCGATTTCCGGCGCGCGGAAACGGCGCCTGCGCCCGG*CTTGTACAGCTCGTCCATG*	76mer
CMV-for	CGCAAATGGGCGGTAGGCGTG	21mer

TABLE 4. Oligonucleotides used for cloning of mNG-UL47 fusion fragments.
Highlighted in grey: NotI cleavage site, double underlined: BglII cleavage site, underlined: (GGGGS)-linker, italic and highlighted in grey: mNG, bold: start codon.

3.1.5 Extraction and purification kits

Kit	Application	Origin	
NucleoSpin® Gel and PCR Clean-up	Gel Extraction	Macherey-Nagel, Oensingen CH	
		http://www.mn-net.com	Cat. No. 740609.250
NucleoSpin® Gel and PCR Clean-up	PCR Clean-up	Macherey-Nagel, Oensingen CH	
		http://www.mn-net.com	Cat. No. 740609.250
QIAprep® Spin Miniprep Kit (250)	Plasmid Miniprep	QIAGEN AG, Hombrechtikon CH	
		https://www.qiagen.com	Cat. No. 27106

TABLE 5. Extraction and purification kits and their origin.
Extraction and purification kits used for cloning of mNG-UL47 fusion fragments.

3.1.6 Bacteria strains

Bacteria strain	Origin	
Escherichia coli TOP 10 F'	Thermo Fisher Scientific - France, Illkirch FR	
	www.thermofisher.com	Cat. No. C303003
Escherichia coli XL-10 gold	Agilent Technologies, Basel CH	
	www.agilent.com	Cat. No. 200314

TABLE 6. *Escherichia coli* strains and their origin.
Escherichia coli strains used for cloning of mNG-UL47 fusion fragments.

3.1.7 Cells

Cells	Features	Origin	
Transfection			
293T	Human primary embryonic kidney cells, highly transfectable, Geneticin resistant	Leibniz-Institut DSMZ-Deutsche Sammlung von Mikroorganismen und Zellkulturen GmbH, Braunschweig DE	
		www.dsmz.de	Cat. No. ACC 635
Transduction and infection			
Leghorn Male Hepatoma (LMH)	Chicken Liver Hepatocellular carcinoma cell line, epithelial	CLS Cell Lines Service GmbH, Eppelheim DE	
		www.clsgmbh.de	Cat. No. 601411

TABLE 7. Cultured cell lines and their origin.
Cells used for transfection or transduction experiments as well as for infection and generation of ILT reporter viruses.

3.1.8 Antibodies

Antibody		Origin	
Western blot			
1st Antibody	rab-α-UL47	Helferich et al., 2007 [36]	
	m-α-GFP	Thermo Fisher Scientific	
		www.thermofisher.com	Cat. No. MA5-15256
2nd Antibody	goat α-rab-HRP	Cell Signaling Technology / Bioconcept, Allschwil CH	
		www.cellsignal.com / www.bioconcept.ch	Cat. No. 7074
	goat α-mouse-HRP	Santa Cruz Biotechnology, Heidelberg DE	
		www.scbt.com	Cat. No. sc-2005
Infection experiment			
goat α-mouse Alexa Fluor 594		Thermo Fisher Scientific	
		www.thermofisher.com	Cat. No. A-11005

TABLE 8. Antibodies and their origin.
Antibodies used for Western blot analysis and infection experiment.

3.1.9 Virus

Virus	Origin
Virulent A-489 ILTV strain	Federal Research Institute for Animal Health', Friedrich-Loeffler-Institut, Greifswald-Insel Riems, Germany

TABLE 9. Virus and its origin.
ILT virus strain used for infection of LMH cells and generation of reporter viruses.

3.2 Methods

3.2.1 Cloning of the mNG-UL47 fusion fragment transfer vectors

3.2.1.1 Amplification and fusion of mNeonGreen and UL47 fragments

In a first polymerase chain reaction (PCR), PCR 1, nine fragments of the UL47 gene were amplified (Fig. 7 PCR 1 A, Fig. 8) according to the protocol listed in table 10. Each amplicon is a particular part of the UL47 gene between 255 bp and 363 bp in length. In parallel, the mNG gene sequence was amplified (Fig. 7 PCR 1 B, Table 10 amplicon A). The overlapping oligonucleotides, listed in table 4, allowed the fusion of the respective UL47 fragment and the amplified mNG in PCR 2 due to complementarity of primer overhangs. One UL47 fragment (UL47_610-622, amplicon 9) consists only of the last twelve C-terminal nucleotides of the entire UL47 gene. This sequence was already included within the primer sequence and thus directly fused to mNG. As template for the different UL47 fragments, high quality purified ILTV DNA was used. pNCS-mNG (Fig. 9) delivered the mNG gene sequence and was therefore used as template for amplicon A.

In addition, mNG was amplified separately, for direct insertion into the expression vector (Fig. 7 PCR 1 B, Table 10 amplicon NG) to serve as mNG expression control in further experiments.

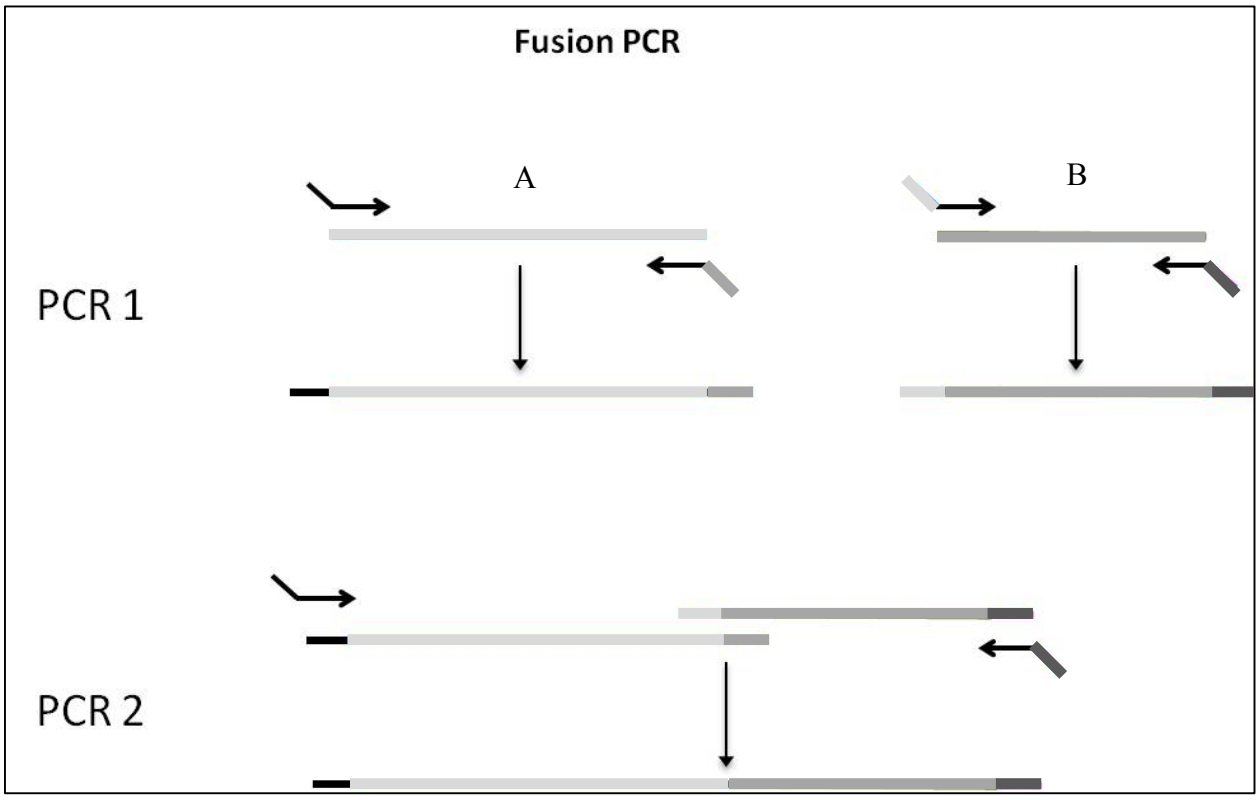

FIG. 7. Scheme of the fusion PCR.
PCR 1 illustrates the annealing of the primers at the particular fragment of UL47 (A) and at the mNG gene sequence respectively (B). The primers contain overlapping parts to enable fusion of the two fragments. PCR 2 shows the fusion of the UL47 fragments with the mNG gene resulting in mNG-UL47 fusion fragments.

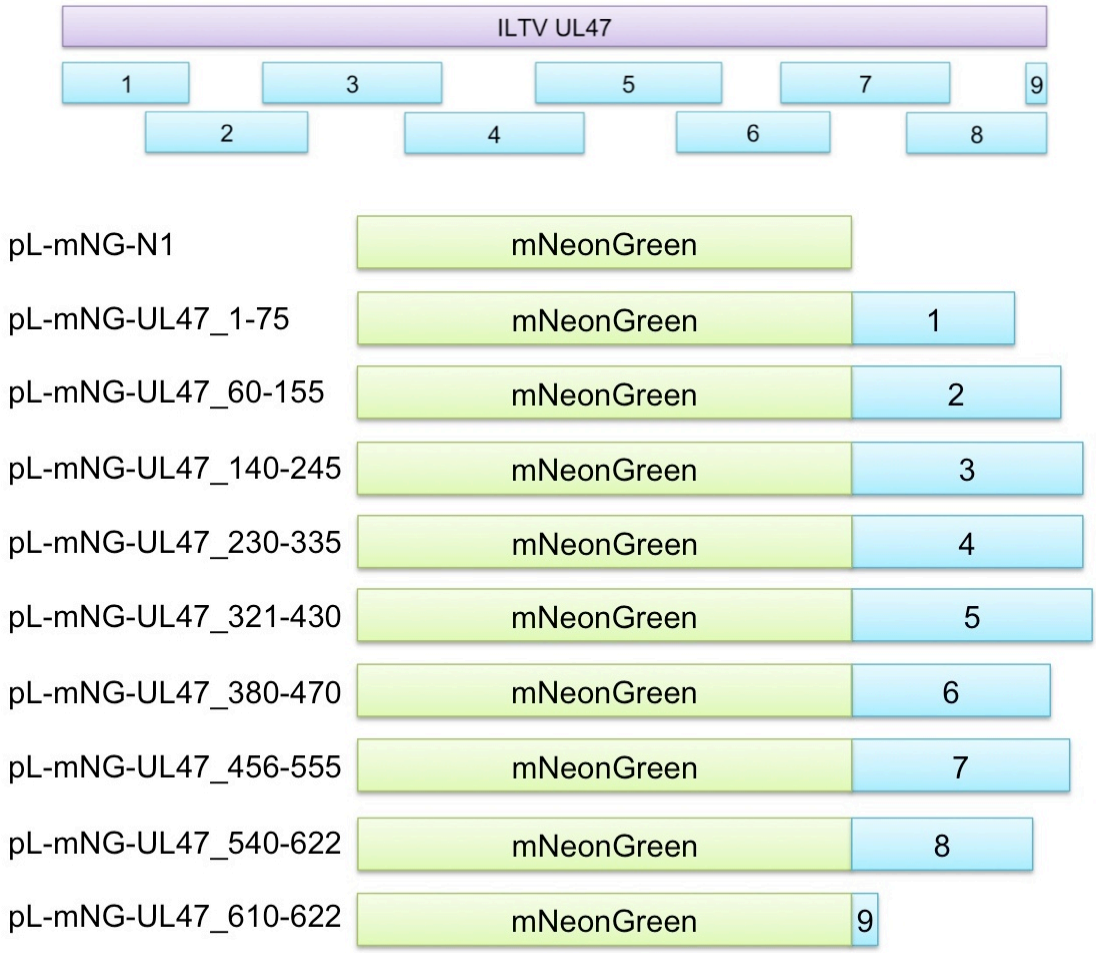

FIG. 8. Scheme of the UL47 fragments 1 to 9, fused to mNG.
Schematic overview of the nine fusion constructs and the pL-mNG-N1 as control for mNG expression. The amplified parts of UL47 are indicated in the name and the length is shown proportionally.

	1	2	3
Template	ILTV DNA	ILTV DNA	ILTV DNA
(+) primer	1UL47_1-75(+)	2UL47_60-155(+)	3UL47_140-245(+)
(-) primer	1UL47_1-75_Not(-)	2UL47_60-155_Not(-)	3UL47_140-245_Not(-)

	4	5	6
Template	ILTV DNA	ILTV DNA	ILTV DNA
(+) primer	4UL47_230-335(+)	5UL47_321-430(+)	6UL47_380-470(+)
(-) primer	4UL47_230-335_Not(-)	5UL47_321-430_Not(-)	6UL47_380-470_Not(-)

	7	8	9
Template	ILTV DNA	ILTV DNA	ILTV DNA
(+) primer	7UL47_456-555(+)	8UL47_540-622(+)	9BglII_mNG(+)
(-) primer	7UL47_456-555_Not(-)	8UL47_540-622_Not(-)	9UL47_610-622_Not(-)

	NG	A
Template	pNCS-mNG	pNCS-mNG
(+) primer	BglII_mNG(+)	BglII_mNG(+)
(-) primer	mNG_Not(-)	mNG(-)

TABLE 10. Templates and primers used for PCR 1. Amplification of UL47 fragments, amplicons A and NG.

Amplicons 1 to 9 represent the nine fragments of the UL47 gene which are supposed to get fused to the mNG gene in a further PCR step. Amplicon NG is generated to serve as control for mNG expression, whereas amplicon A was used for fusion to the respective UL47 fragments in PCR 2.

Reaction mixtures for PCR 1 were pipetted according to following protocol:

50 ng template
10 µl 5x Phusion HF Buffer
1 µl dNTP (10 mM)
2 µl Primer (+) (10 mM)
2 µl Primer (-) (10 mM)
0.5 µl Phusion DNA polymerase
add H_2O to total volume of 50 µl

For all reactions of PCR 1, identical thermocycling conditions were applied (Table 11 A). For fragment 9, the annealing temperature was modified by alteration to 44°C for 30 s (marked bold in Table 11 B). The thermocycling was performed in a 2720 thermal cycler (Applied Biosystems, Foster City, CA, USA).

Each amplicon was verified by electrophoresis on a 1% agarose gel supplemented with 0.02% ethidium bromide (EtBr) in TAE buffer. The electrophoresis was run for 90 to 120 min with 100 V DC (direct current). As reference the 1 kb Plus DNA Ladder was used. The bands were visualized and photographed by using the AlphaImager™ Gel Imaging System.

A)

98°C	1’	
98°C	0.5’	25 x
46°C	0.5’	
72°C	0.5’	
72°C	5’	
4°C	∞	

B)

98°C	1’	
98°C	0.5’	25 x
44°C	0.5’	
72°C	0.5’	
72°C	5’	
4°C	∞	

TABLE 11. Thermocycling conditions PCR 1.
Thermocycling conditions for the amplification of UL47 fragments 1 to 8, amplicon A and NG (A) as well as for UL47 fragment 9 (B). The modification is highlighted in bold.

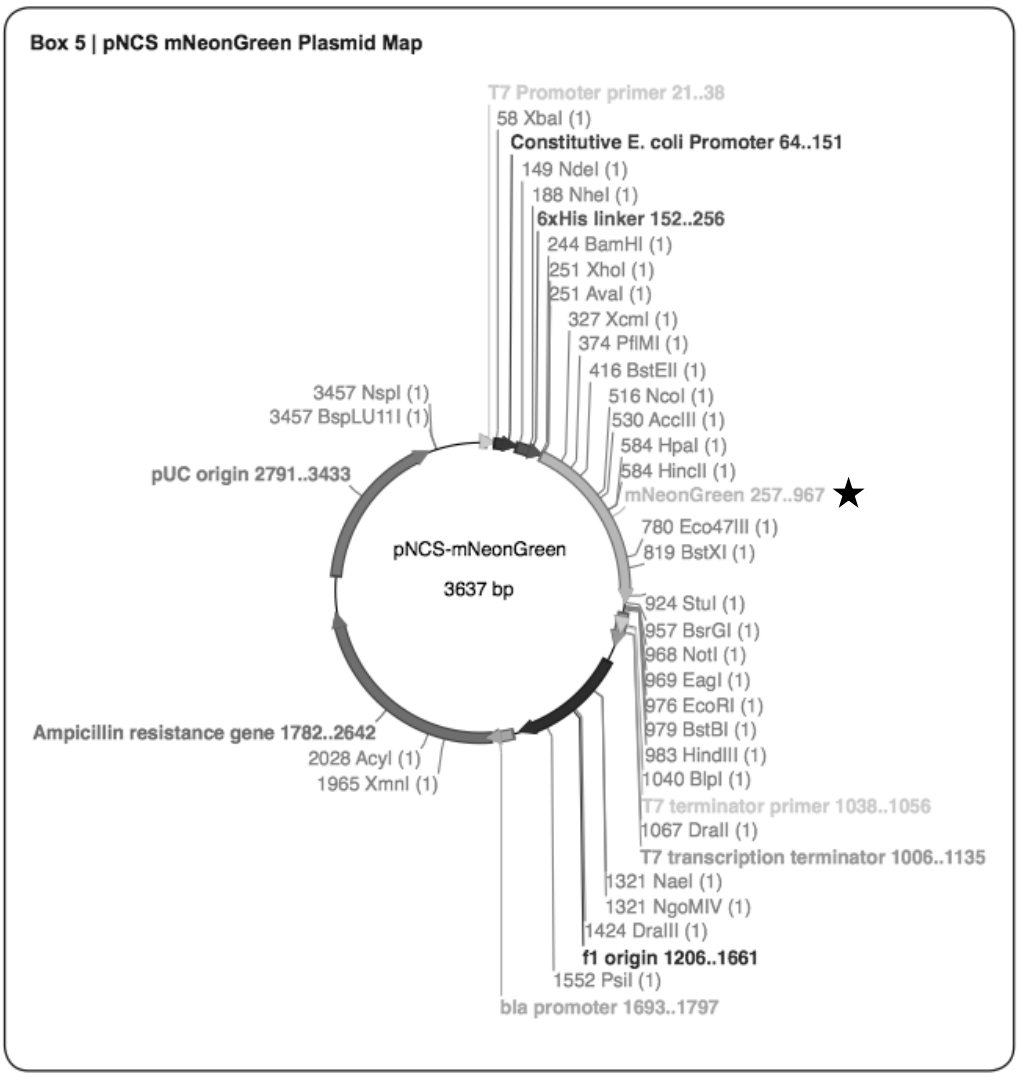

FIG. 9. Map of pNCS-mNeonGreen plasmid, Allele Biotechnology, San Diego, CA, USA. The plasmid pNCS-mNeonGreen was used as template for the amplification of both mNG fragments (amplicon A, amplicon NG). mNeonGreen is marked with a star.

In a second PCR mNG (amplicon A) was fused to the respective UL47 fragment (amplicon 1 - 8) (Fig. 7 PCR 2, Fig. 8) according to the protocol listed in table 12. The UL47 fragment 9 sequence (UL47-610_622) is included within the primer and was already fused to mNG in PCR 1. Therefore, no further PCR step was necessary for this particular fragment.

	A1	A2	A3
Templates	A	A	A
	1	2	3
(+) primer	BglII_mNG(+)	BglII_mNG(+)	BglII_mNG(+)
(-) primer	1UL47_1-75_Not(-)	2UL47_60-155_Not(-)	3UL47_140-245_Not(-)

	A4	A5	A6
Templates	A	A	A
	4	5	6
(+) primer	BglII_mNG(+)	BglII_mNG(+)	BglII_mNG(+)
(-) primer	4UL47_230-335_Not(-)	5UL47_321-430_Not(-)	6UL47_380-470_Not(-)

	A7	A8
Templates	A	A
	7	8
(+) primer	BglII_mNG(+)	BglII_mNG(+)
(-) primer	7UL47_456-555_Not(-)	8UL47_540-622_Not(-)

TABLE 12. Templates and primers used for PCR 2. Amplification of mNG-UL47 fusion fragments A1 to A8.

mNG amplified in PCR 1 (amplicon A) and the respective UL47 fragments (amplicon 1-8) were used to generate mNG-UL47 fusion fragments.

Reaction mixtures for PCR 2 were pipetted according to following protocol:

50 ng amplicon A
other templates as follows:

1: 17 ng	2: 22 ng	3: 24 ng	4: 24 ng	5: 25 ng	6: 21 ng	7: 23 ng	8: 20 ng

10 µl 5x Phusion HF Buffer
1 µl dNTP (10 mM)
2 µl Primer (+) (10 mM)
2 µl Primer (-) (10 mM)
0.5 µl Phusion DNA polymerase
add H_2O to total volume of 50 µl

For all reactions of PCR 2, identical thermocycling conditions were applied (Table 13). The thermocycling was performed in a 2720 thermal cycler (Applied Biosystems, Foster City, CA, USA).

98°C	1’	
98°C	0.5’	25 x
46°C	0.5’	
72°C	1’	
72°C	5’	
4°C	∞	

TABLE 13. Thermocycling conditions PCR 2.
Thermocycling conditions for the amplification of mNG-UL47 fusion fragments A1 to A8.

Each mNG-UL47 fusion fragment was verified by electrophoresis as described above.

Amplicons were purified after the first and second PCR using the NucleoSpin® Gel and PCR Clean-up Kit (Table 5). Concentrations and purities were measured using the NanoDrop spectrophotometer (Witec AG, Littau, Switzerland. Data not shown).

3.2.1.2 Enzymatic restriction of mNG-UL47 fusion fragments and expression vector

mNG-UL47 fusion fragments were enzymatically digested according to following protocol:

Whole eluate (40 µl or 90 µl respectively)
10 µl NEB buffer 3.1
1 µl BglII
1 µl NotI

The reaction was incubated for 2 h at 37°C and subsequently purified using the NucleoSpin® Gel and PCR Clean-up Kit (Table 5). Concentrations and purities of these mNG-UL47 fusion fragments were measured using the NanoDrop spectrophotometer (Witec AG, Littau, Switzerland. Data not shown).

The purified mNG-UL47 fusion fragments were inserted into expression vector pL-EGFP-N1 (Fig. 10) by ligation. This vector was previously digested according to following protocol:

2 µg pL-EGFP-N1
10 µl NEB buffer 3.1
2 µl NotI
1 µl BglII
add H_2O to total volume of 100 µl

The mixture was incubated for 2 h at 37°C and subsequently verified by electrophoresis as described in chapter 3.2.1.1. The band with the specific size of the desired fragment was excised from the agarose gel, extracted and purified. The obtained concentration was measured as described above.

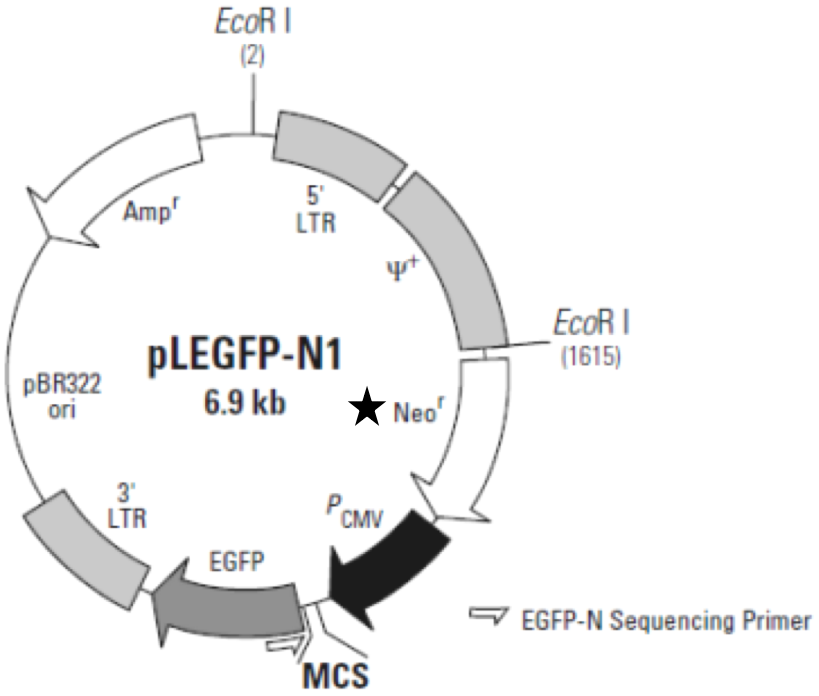

FIG. 10. Map of pL-EGFP-N1 plasmid, BD Biosciences Clontech, Protocol PT3233-5, Version PR29959.

The retroviral vector pLEGFP-N1 serves as expression vector. It was digested using NotI and BglII resulting in the excision of EGFP. It carries two antibiotic resistant genes, Neo^r and Amp^r, whereas the essential one for selection of eukaryotic cells is Neo^r, which is marked with a star.

3.2.1.3 Ligation

The ligation reaction using a molar ratio of 1:3 (insert:vector) was prepared corresponding to table 14. The retroviral vector pL-EGFP-N1 served as expression vector, inserts were the various mNG-UL47 fusion fragments and mNeonGreen only. 10 mM dATP was supplemented. Reactions were incubated over night at 16°C or for 10 min at 22°C. To inactivate the ligation complexes, the temperature was raised to 65°C for 15 min, followed by cooling down to room temperature (RT). 0.5 µl BamHI was pipetted to each reaction which was subsequently incubated for 45 min at 37°C. This step was included for linearization of circular, non-restricted vector plasmids. Two negative controls were prepared according to table 14 (Neg. Ctr. 1 and Neg. Ctr. 2). Both contained no inserts (control for unspecific ligation of the restricted vector) and Ctr. 2 in addition was lacking the T4 ligase (control for uncut vector).

	Neg. Ctr. 1	Neg. Ctr. 2	pL-mNG-N1	pL-mNG-UL47 _1-75
Vector DNA	30 ng	30 ng	30 ng	30 ng
Insert DNA	---	---	10 ng	10 ng
NEB buffer 3.1	1 µl	1 µl	1 µl	1 µl
dATP	1 µl	1 µl	1 µl	1 µl
T4 ligase	0.5 µl	---	0.5 µl	0.5 µl
Add H_2O to a total volume	10 µl	10 µl	10 µl	10 µl

	pL-mNG-UL47 _60-155	pL-mNG-UL47 _140-245	pL-mNG-UL47 _230-335	pL-mNG-UL47 _321-430
Vector DNA	30 ng	30 ng	30 ng	30 ng
Insert DNA	10 ng	5 ng	5 ng	5 ng
NEB buffer 3.1	1 µl	1 µl	1 µl	1 µl
dATP	1 µl	1 µl	1 µl	1 µl
T4 ligase	0.5 µl	0.5 µl	0.5 µl	0.5 µl
Add H_2O to a total volume	10 µl	10 µl	10 µl	10 µl

	pL-mNG-UL47 _380-470	pL-mNG-UL47 _456-555	pL-mNG-UL47 _540-622	pL-mNG-UL47 _610-622
Vector DNA	30 ng	30 ng	30 ng	30 ng
Insert DNA	5 ng	5 ng	5 ng	5 ng
NEB buffer 3.1	1 µl	1 µl	1 µl	1 µl
dATP	1 µl	1 µl	1 µl	1 µl
T4 ligase	0.5 µl	0.5 µl	0.5 µl	0.5 µl
Add H_2O to a total volume	10 µl	10 µl	10 µl	10 µl

TABLE 14. Mixtures of ligation reactions using a 1:3 molar ratio. Two negative controls (Neg. Ctr. 1 and Neg. Ctr. 2) were included.

3.2.1.4 Transformation of chemical competent *E. coli* and purification of plasmid DNA

Escherichia coli TOP 10 F' and *Escherichia coli* XL-10 gold (Table 6) were used for transformation of ligated vectors. Prepared aliquots of 50 µl were thawed on ice. 5 µl of the ligation reaction was added and incubated on ice for 30 min. The bacteria were heatshocked for 30 seconds in a 42°C water bath and placed back on ice. 250 µl S.O.C medium was pipetted into each vial followed by horizontally shaking with 200 rpm at 37°C for 1 h. Subsequently, the entire content of each vial was plated onto LB-agar-plates which were supplemented with ampicillin and incubated over night at 37°C.
The following day, the grown bacteria colonies were counted and five colonies of each LB-agar-plate were collected for plasmid isolation using the QIAprep® Spin Miniprep Kit (250) (Table 5).

3.2.1.5 Control restriction analysis

The digestions of newly generated plasmids harbouring the mNG-UL47 fusion fragments were done according to following protocol:

500 ng DNA
1 µl Buffer 0
0.5 µl Eco47III
add H_2O to total volume of 10 µl

The reaction mixture was incubated for 1 h at 37°C and subsequently verified by electrophoresis as described in chapter 3.2.1.1.

3.2.2 Transfection

3.2.2.1 Transfection of 293T cells

293T cells were cultured in DMEM (Dulbecco's modified eagle medium) supplemented with 9% fetal bovine serum (FBS) and Penicillin-Streptomycin (P/S) (100 U/ml penicillin / 0.1 mg/ml streptomycin) to an approximately 90% confluent cell layer in a 10 cm dish. After detaching and resuspending the cells in 7.5 ml DMEM, cells were counted using a Neubauer improved cell counting chamber and adjusted to a final concentration of 2 x 10^5 cells per ml. Cells were seeded in a 12-well plate, 1 ml per well. 24 h after seeding, the 293T cells were transfected by lipofection using *Trans*IT-2020 as transfection reagent. For generation of retroviral vectors, the packaging construct pHit60, the envelope construct pMD2.G and one of the newly generated mNG-UL47 fusion fragment transfer vectors were co-transfected into 293T cells using the following mixture:

100 µl OptiMEM
0.6 µg transfer vector
0.4 µg pHit60
0.2 µg pMD2.G
3 µl *Trans*IT-2020

As negative control, 293T cells were transfected with OptiMEM and *Trans*IT-2020 only. The transfection mixture was incubated for 20 min at RT. The medium was replaced with 1 ml DMEM containing neither FBS nor antibiotics and the transfection mix was gently and dropwise added to the cells in the 12-well plate. Following incubation at 38°C and 5% CO_2 for 4 h, 11 µl P/S were pipetted to each well. After approximately 24 h of incubation at 38°C and 5% CO_2, all wells were monitored for fluorescence.

3.2.2.2 Monitoring immunofluorescence of 293T cells

About 24 h and 48 h post-transfection, the immunofluorescence of transfected 293T cells was monitored with a Zeiss light microscope (Axiovert 25) and compared to the negative control. The fluorescence intensity and quantity within each well was assessed subjectively by a rating scheme with values negative (-), low (+), moderate (++) or high (+++) at 48 h post-transfection.

3.2.3 Transduction

3.2.3.1 Transduction of LMH cells

7×10^5 LMH cells per well were seeded in 6-well plates and were cultivated in 2 ml Waymouth's medium supplemented with 9% FBS and P/S (100 U/ml penicillin / 0.1 mg/ml streptomycin). The next day, retroviral vector-containing supernatant (SN) of transfected 293T cells was harvested and filtered through a 0.45 µm PES-membrane filter. 1 ml of the yield was directly added to the respective LMH cells. To increase transduction efficiency, Polybrene was added in a final concentration of 1 ng/ml to each well. Polybrene is a cationic polymer which is supposed to enhance retrovirus-mediated gene transfer [37], [38]. As retroviruses can only infect/transduce growing cells [39], [40] and Polybrene has toxic effects on cells depending on the time of exposure and concentration [41], the appropriate amount and incubation time was determined in advance. The 6-well plates were centrifuged with 2500 rpm for 30 min at RT, followed by incubation at 38°C and 5% CO_2 for 5 h. Thereafter, LMH cells were washed carefully with 1 ml Dulbecco's phosphate buffered saline (PBS) and the medium was replaced with Waymouth's medium supplemented with 9% FBS and P/S (100 U/ml penicillin / 0.1 mg/ml streptomycin). After 24 h of incubation at 38°C and 5% CO_2, all wells were monitored for fluorescence.

3.2.3.2 Monitoring immunofluorescence of LMH cells

A subset of cells was grown on cover slips. After fixation with 3% paraformaldehyde (PFA) and staining of the nuclei with DAPI, cells were monitored for expression and localization of the mNG-UL47 fusion proteins by using an Olympus IX81 inverted epifluorescence microscope. DIC and fluorescent images were taken at 60x magnification.

3.2.3.3 Antibiotic selection

Cells stably expressing the mNG-UL47 fusion proteins were selected by using G418 (Geneticin), an aminoglycoside antibiotic. It inhibits the protein synthesis in prokaryotic and eukaryotic cells likewise. The resistance to G418 is conferred by the Neomycin resistant gene (Neo^r, Fig. 10) [42]. Due to the presence of Neo^r on the newly generated transfer vectors, cells, which express the UL47-mNG fusion proteins, are also supposed to express the Neomycin resistance gene and therefore be unsusceptible to antibiotic treatment with G418.

3.2.4 Western blot

3.2.4.1 Western blot of UL47 fusion proteins

To demonstrate the incorporation and successful expression of the mNG-UL47 fusion fragments in 293T cells, Western blot analysis was performed.

In a 25 cm^2 cell culture flask 293T cells were cultured in DMEM supplemented with 9% FBS and and P/S (100 U/ml penicillin / 0.1 mg/ml streptomycin) to a density of approximately 90%. After detaching and resuspending the cells in 7.5 ml DMEM, cells were counted using a Neubauer improved cell counting chamber and adjusted to a final concentration of 2 x 10^5 cells per ml per well. Cells were seeded in a 12-well plate, 1 ml per well. 24 h after seeding, the 293T cells were transfected by lipofection using the *Trans*IT-2020 transfection reagent according to following protocol:

100 µl OptiMEM
1 µg DNA
3 µl *Trans*IT-2020

The transfection mixture was incubated for 20 min at RT. The medium was replaced with 1 ml DMEM containing neither FBS nor antibiotics and the transfection mix was gently and dropwise added to the cells in the 12-well plate. Following incubation at 38°C and 5% CO_2 for 4 h, 11 µl P/S was pipetted to each well. After 24 h of incubation at 38°C and 5% CO_2 the cells were washed with PBS. 1 ml PBS was added to each well and cells were scraped of and transferred to Eppendorf tubes. Subsequently, the cells were spun down with 10'000 rpm for 10 min at RT and thereupon the pellets were lysed using RIPA lysis buffer.

To determine the protein concentration, the Bradford Protein Assay method [43] was used.

15 µg of obtained lysates were incubated at 95°C for 5 min together with Lämmli buffer and loaded onto a 10% SDS polyacrylamide gel. The gel ran 30 min with 50 V followed by 100 V for 90 min according to standard SDS PAGE protocol in the Mini-PROTEAN® Tetra System (Bio-Rad).

The blotting was performed with the Trans-Blot® SD Semi-Dry Electrophoretic Transfer Cell (Bio-Rad) with 20 V for 1 h. Before blotting, filter papers and nitrocellulose membranes were soaked in blotting buffer and thereafter assembled on the cathode plate together with the gel, carefully to avoid air bubbles. To prevent unspecific antibody binding, membranes were blocked for 1 h while shaking at RT using 5% milk powder in Tris-buffered saline (TBS).

Nitrocellulose membranes were incubated with the primary antibody (rab-α-UL47, 1:10'000 or m-α-GFP, 1:5'000 in 2.5% milk powder in TTBS) at 4°C shaking over night. The next day, nitrocellulose membranes were washed three times with TTBS for 5 min each at RT shaking. Incubation with the secondary antibody (goat α-rab-HRP or goat α-mouse-HRP,

1:1000 in 2.5% milk powder in TTBS) was done at RT for 1 h shaking and followed by a washing step with TTBS and two times washing with TBS for approximately 10 min each. For detection, the membranes were incubated with enhanced chemiluminescence (ECL) reagent for 2 min. Subsequently, they were exposed to Fuji Medical X-ray film 100 NIF with different exposure times, 1, 5 or 15 min. The films were developed using the Agfa Curix 60 (Schenk AG, Hettlingen CH).

3.2.5 Infection of LMH cells and generation of ILT reporter viruses

3.2.5.1 Generation of ILT reporter viruses and microscopic analysis

Generated LMH cell lines with incorporated mNG-UL47 fusion fragments were cultured in 10 cm dishes in Waymouth's medium supplemented with 10% FBS at 38°C and 5% CO_2. 48 h after seeding, cells were infected with a mutant ILTV lacking the UL47 gene (ILTV-ΔUL47). Incubation of infected cells lasts till a cytopathic effect was observed. Viral particles were collected, filtered through a 0.45 µm filter and subsequently concentrated by centrifugation for 1 h at 48'000x g (supernatant was discarded and particles were resuspended in 200 µl PBS). For microscopic analysis, glass coverslips (cs) were coated with 0.01% Poly-L-lysine solution for 1 h at RT. The cs were washed twice with ddH_2O. For binding, 100 µl of virus solution was added per cs and incubated for 1 h at RT. The virus solution was aspirated and cs were washed once with PBS. Viruses were fixated with 3% PFA. After blocking with 10% goat serum for 30 min at RT, cs were incubated with an antibody recognizing the ILTV glycoprotein J (gJ) (1:50 in 10% goat serum) for 1 h at RT. After washing three times with PBS, the cs were incubated with α-mouse-AlexaFluor 594 for 1 h at RT in the dark. This was followed by washing twice with PBS and mounting of the cs onto microscope slides. Images were recorded with 100x magnification with the Zeiss Axiovert Observer Z1 microscope. The amount of fluorescence spots was subjectively rated by a rating scheme with values negative (-), low (+), moderate (++) or high (+++).

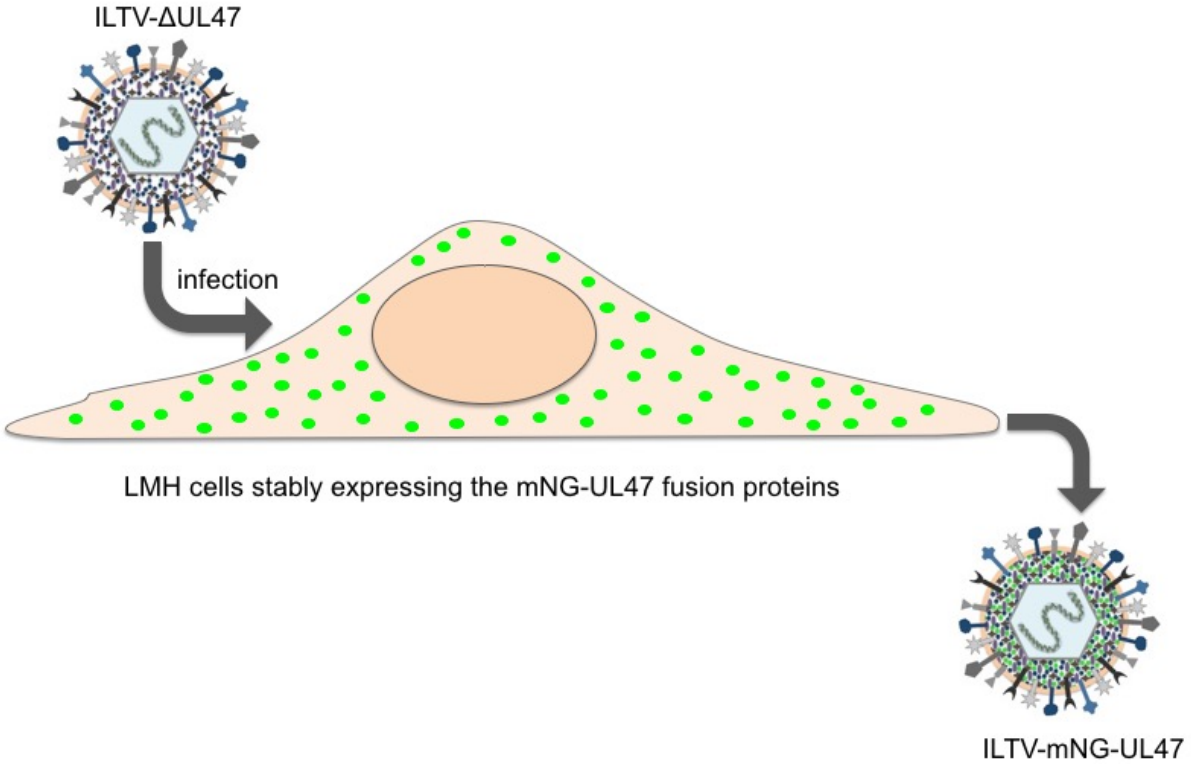

FIG. 11. Scheme of the generation of ILT reporter viruses.
LMH cells were infected with mutant ILTV that lacks the wild type UL47 protein. Subsequent propagation of reporter virus with incorporated mNG-UL47 fusion fragments.

4. Results

4.1 Cloning of the mNG-UL47 fusion fragment transfer vectors

Amplification and fusion of the respective UL47 fragments to mNG was successfully achieved. This was shown by gel electrophoresis as described in chapter 3.2.1.1 (Fig. 12, 13 and Table 15, 16).

The products of the first PCR appeared as distinct bands with the correct sizes (Table 15, Fig. 12, A, B, C), while UL47 fragment 9 delivered a blurred band (Fig. 12, B). Hence, a modified cycler program with a decreased annealing temperature of 44°C (Table 11, B) was run for fragment 9, resulting in a more distinct signal (Fig. 12, D).

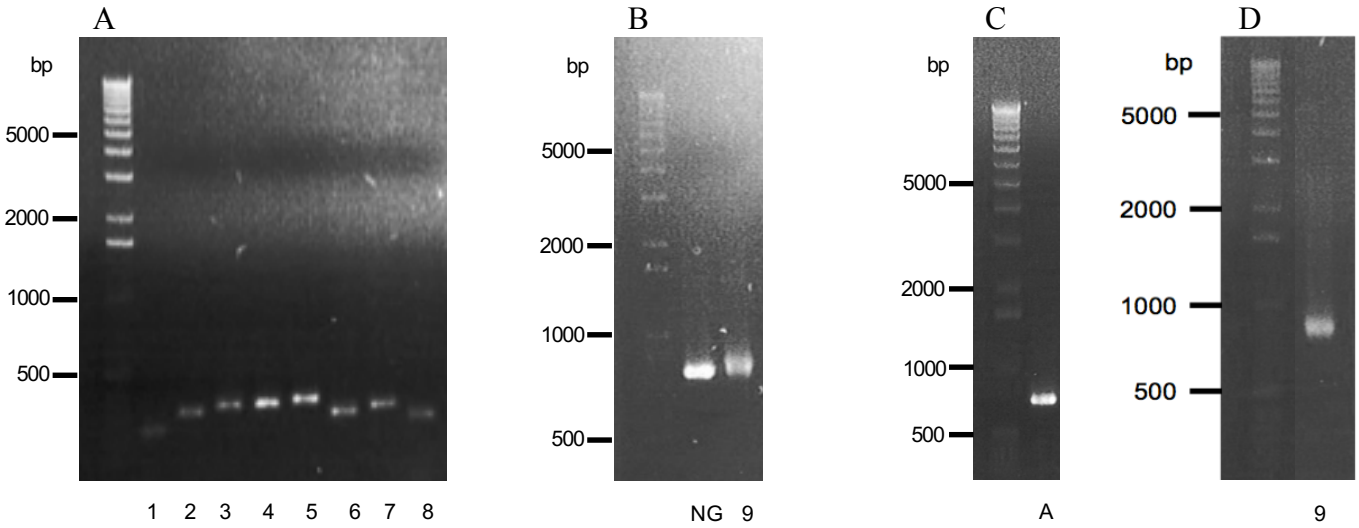

FIG. 12. PCR 1. Amplification of nine UL47 fragments and two mNG gene sequences. 1% agarose gel.
A: UL47 fragments 1-8, B: mNeonGreen (NG) for cloning the expression control plasmid and UL47 fragment 9 directly fused to mNG, C: mNeonGreen for fusion to the UL47 fragments (A), D Amplicon 9 repeated with a modified cycler program.

Fragment	1	2	3	4	5	6	7	8	9	A	NG
Size (bp)	255	321	351	351	363	306	333	288	787	739	742

TABLE 15. Expected band sizes of amplicons of PCR 1.
UL47 fragments 1 to 8, mNeonGreen (A and NG).

In the second PCR the UL47 fragments one to eight were fused to the mNG sequence. The fusion fragments appeared at the expected molecular weight size (Fig. 13, Table 16). Weak bands of smaller size were visible.

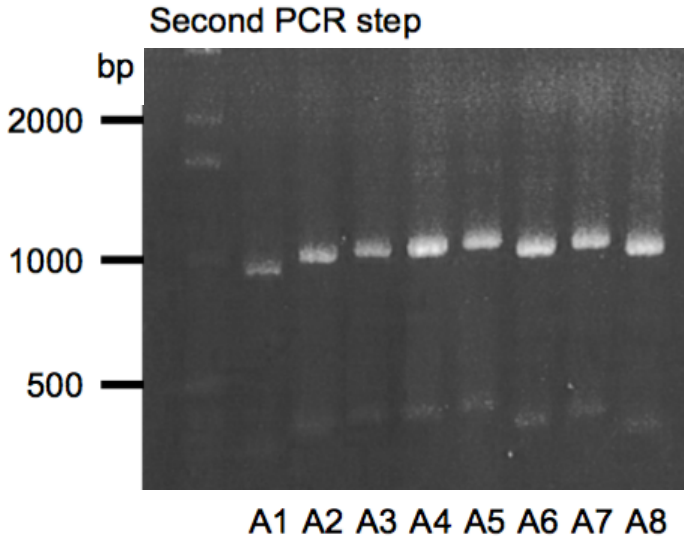

FIG. 13. PCR 2. Amplification of fusion fragments A1 to A8.
Fusion of UL47 fragments 1 – 8 to mNG. 1% agarose gel.

Fusion fragment	A1	A2	A3	A4	A5	A6	A7	A8
Size (bp)	979	1045	1075	1075	1087	1030	1057	1012

TABLE 16. Expected band sizes of amplicons of PCR 2.
UL47 fragments fused to mNG (A1 to A8).

Digestion of the expression vector with the respective restriction enzymes was controlled by electrophoresis as described in chapter 3.2.1.1 (Fig. 14 and Table 17). Bands corresponding to 6129 bp were excised from the agarose gel, extracted and purified.

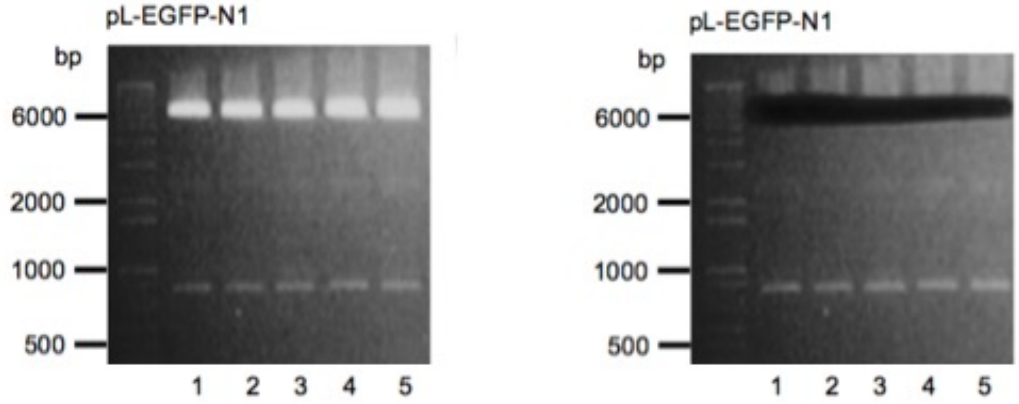

FIG. 14. Restriction of pL-EGFP-N1 and isolation of the vector backbone. 1% agarose gel. The 100 µl restriction reaction was loaded into 5 pockets of the gel (lane 1 - 5). A. before and B. after excision of the vector backbone.

Expression vector	**Restriction enzyme**	**Expected band sizes**	
pL-EGFP-N1	NotI and BglII	762 bp	6129 bp

TABLE 17. Restriction enzyme analysis of the vector backbone.
Expected band size after restriction with NotI and BglII.

mNG-UL47 fusion fragments were restricted using the same restriction enzymes (NotI and BglII). Upon purification, the fusion fragments were ligated into the vector backbone and the resulting plasmids were transformed into chemical competent *Escherichia coli.* The bacteria strains used for transformation and the number of colonies counted 24 h after transformation are listed in table 18.

Construct	**Number of colonies**	***Escherichia coli* strain**
Negative control 1	0 / 0	TOP 10 F' / XL-10 gold
Negative control 2	0 / 5	TOP 10 F' / XL-10 gold
pL-mNG-N1	12	XL-10 gold
pL-mNG-UL47_1-75	204	XL-10 gold
pL-mNG-UL47_60-155	72	XL-10 gold
pL-mNG-UL47_140-245	8	TOP 10 F'
pL-mNG-UL47_230-335	9	TOP 10 F'
pL-mNG-UL47_321-430	9	TOP 10 F'
pL-mNG-UL47_380-470	7	TOP 10 F'
pL-mNG-UL47_456-555	21	TOP 10 F'
pL-mNG-UL47_540-622	30	TOP 10 F'
pL-mNG-UL47_610-622	9	XL-10 gold

TABLE 18. Amount of bacterial colonies.
Colonies grown on LB-Amp-plates after transformation of the newly generated expression vectors into competent *Escherichia coli* colonies.

Five *Escherichia coli* colonies of each construct were picked and grown in LB-Amp medium. Plasmid DNA was isolated and correct cloning was verified by restriction enzyme analysis and subsequent DNA sequencing (Fig. 15). The restriction enzyme was equal for all generated constructs. Eight out of nine mNG-UL47 expression vectors showed the expected band sizes (Table 19). Restriction of mNG-UL47_610-622 did not result in correct band patterns in any analysed sample (Fig. 15).

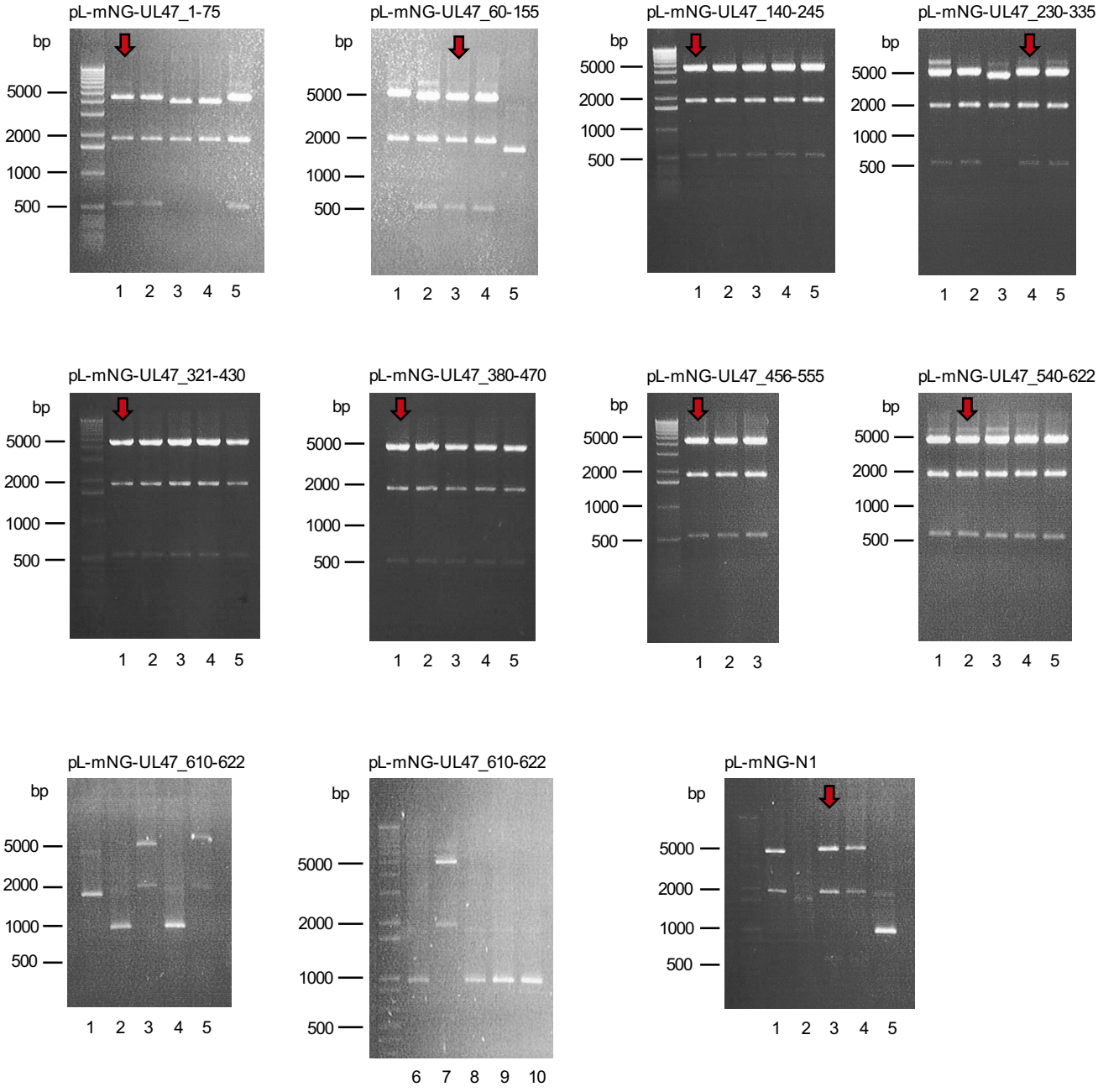

FIG. 15. Restriction enzyme analysis of newly generated UL47-mNG expression vectors. 1% agarose gel.

For each construct, five samples were analysed (lanes 1-5). Due to a lack of correct samples, additional five plasmids of pL-mNG-UL47_610-622 were analysed. Samples marked with an arrow were verified by sequencing and use for further investigation.

Construct	Size (bp)		
pL-mNG-N1	549	1924	4352
pL-mNG-UL47_1-75	549	1924	4589
pL-mNG-UL47_60-155	549	1924	4655
pL-mNG-UL47_140-245	549	1924	4685
pL-mNG-UL47_230-335	549	1924	4685
pL-mNG-UL47_321-430	549	1924	4697
pL-mNG-UL47_380-470	549	1924	4640
pL-mNG-UL47_456-555	549	1924	4667
pL-mNG-UL47_540-622	549	1924	4622

TABLE 19. Restriction enzyme analysis of generated constructs.
Expected band size after restriction with Eco47III.

4.2 Transfection – Generation of retroviral vectors in 293T cells

48 h after transfection, immunofluorescence was examined and resulted in the following observations: the negative control showed no fluorescence. Transfection of six out of nine mNG-UL47 expression constructs, namely pL-mNG-N1, pL-mNG-UL47_60-155, pL-mNG-UL47_230-335, pL-mNG-UL47_321-430, pL-mNG-UL47_380-470 and pLmNG-UL47_540-622 resulted in a high fluorescence intensity and quantity, as listed in table 20 A. Transfection of pL-mNG-UL47_1-75 and pL-mNG-UL47_456-555 showed moderate fluorescent intensity and quantity while transfection of pL-mNG-UL47_140-245 resulted in a few cells showing moderate fluorescent intensity (Table 20 A). Therefore, the transfection was repeated for those three constructs using double amounts of the respective transfer vectors. Fluorescence resulting from transfection of pL-mNG-UL47_1-75 remained unchanged. Upon transfection of pL-mNG-UL47_140-245 the amount of fluorescent cells increased slightly but with unchanged intensity, while transfection of pL-mNG-UL47_456-555 showed slightly higher rates of both, fluorescence intensity and quantity (Table 20 B).

A

mNG-UL47 transfer vector	Fluorescence intensity	Fluorescence quantity
Negative control	-	-
pL-mNG-N1	+++	+++
pL-mNG-UL47_1-75	++	++
pL-mNG-UL47_60-155	+++	+++
pL-mNG-UL47_140-245	+/++	+
pL-mNG-UL47_230-335	+++	+++
pL-mNG-UL47_321-430	+++	+++
pL-mNG-UL47_380-470	+++	+++
pL-mNG-UL47_456-555	++	++
pL-mNG-UL47_540-622	+++	+++

B

mNG-UL47 transfer vector	Fluorescence intensity	Fluorescence quantity
Negative control	-	-
pL-mNG-UL47_1-75	++	++
pL-mNG-UL47_140-245	+/++	+/++
pL-mNG-UL47_456-555	++/+++	++/+++

TABLE 20. Results of transfection of fusion fragment transfer vectors subjectively rated with scores for fluorescence intensity and quantity 48 h post-transfection

Rating scheme of the observed fluorescence: negative: -, low: +, moderate: ++, high: +++; Table A: first approach of transfection. Table B: Repetition of transfections with suboptimal performance scores, double amounts of plasmids used.

4.3 Analysis of LMH cells stably expressing various mNG-UL47 fusion proteins

A subset of stably transduced LMH cells was fixed with PFA and nuclei were stained with DAPI. These cells were examined for the expression and localization of the mNG-UL47 fusion proteins (Fig. 16).

LMH cells:
Native LMH cells served as negative control. No neon green fluorescence was detectable besides some blurred background or auto-fluorescence.
mNG-N1:
Neon green fluorescence was detectable mainly within the nuclei and and with lower intensity also in the cytosol.
mNG-UL47_1-75:
No green fluorescence signal was detectable (data not shown). Therefore, the construct was not used for further investigation
mNG-UL47_60-155:
Neon green fluorescence was detectable within the nuclei and with similar intensity also in the cytosol.
mNG-UL47_140-245:
A faint neon green fluorescence was detectable within the nuclei and the cytoplasm. Noticeable, bright fluorescent spots appeared in close proximity to the nuclei.
mNG-UL47_230-335:
Neon green fluorescence was detectable within the nuclei and with similar intensity also in the cytosol.
mNG-UL47_321-430:
Very few cells showed a fluorescent signal in form of very bright distinct spots.
mNG-UL47_380-470:
Neon green fluorescence was detectable within the nuclei and very bright distinct spots were observed in the cytosol, like they were detected for mNG-UL47_321-430.
mNG-UL47_456-555:
Neon green fluorescence was detectable within the nuclei and the cytosol. Furthermore, very bright distinct spots were observed in the cytosol, similar to those detected for mNG-UL47_321-430.
mNG-UL47_540-622:
Neon green fluorescence was detectable mainly within the nuclei.

Neon green fluorescence	DAPI counterstain	Merged images
LMH cells		
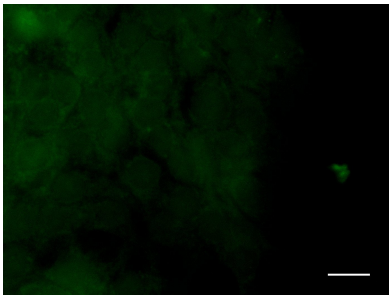	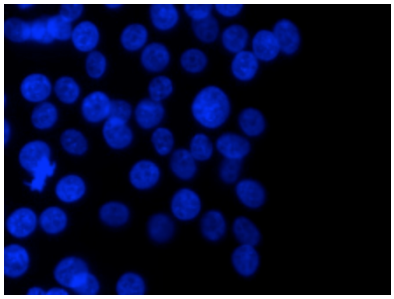	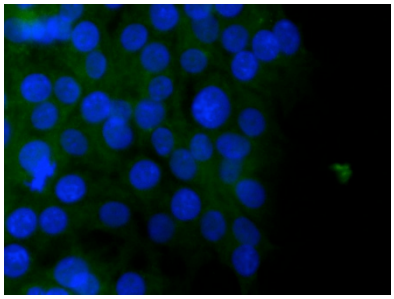
construct **pL-mNG-N1**		
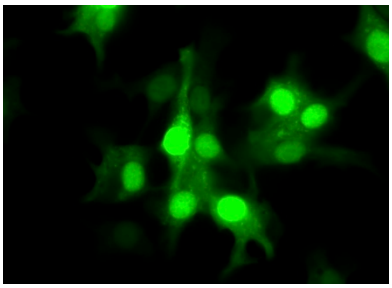	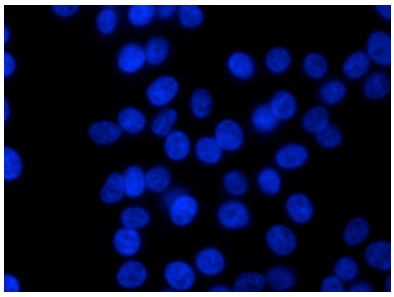	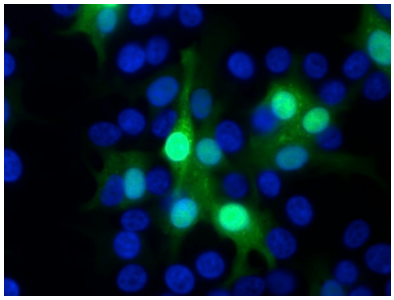
construct **pL-mNG-UL47_60-155**		
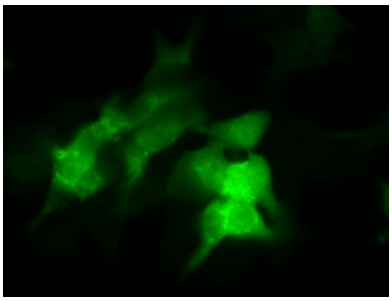	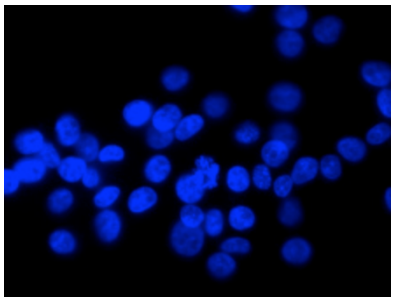	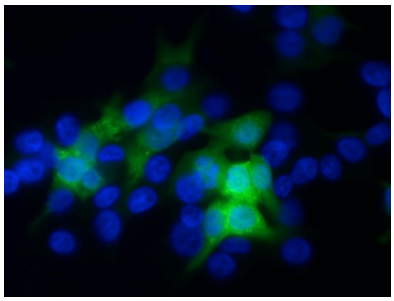
construct **pL-mNG-UL47_140-245**		
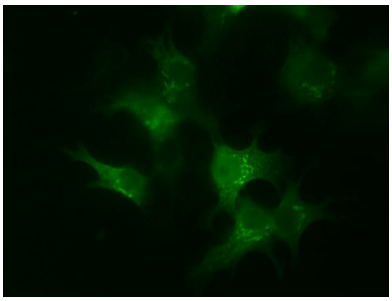	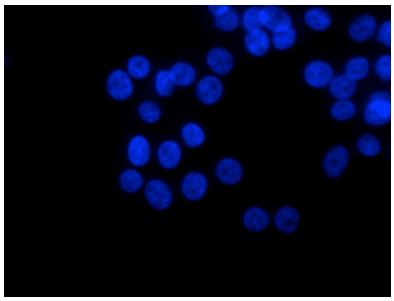	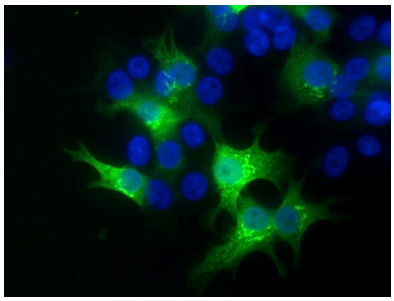
construct **pL-mNG-UL47_230-335**		
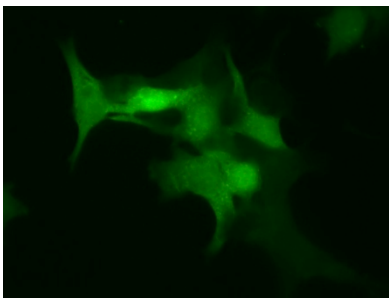	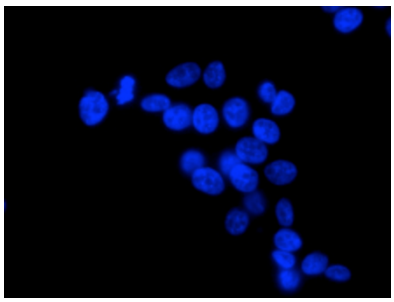	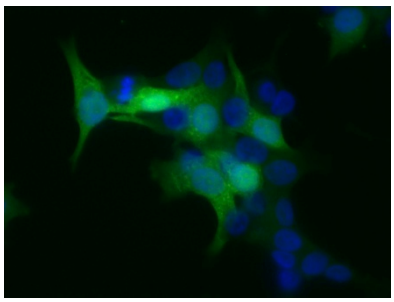

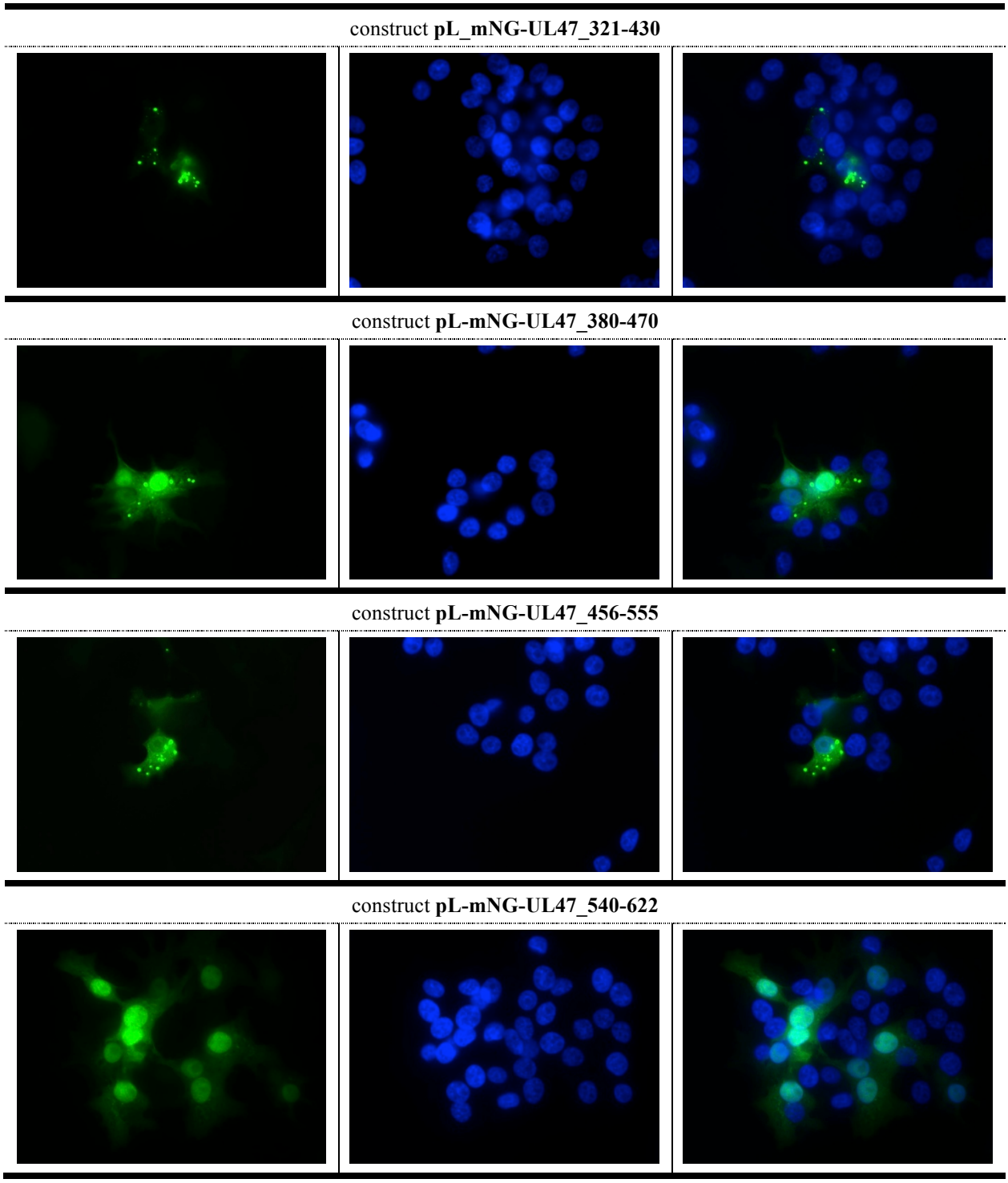

FIG. 16. Expression and localization of various mNG-UL47 fusion proteins.
left: green – mNG or mNG-UL47 fusion proteins, middle: blue – DAPI, right: merge. 60x magnification. Scale bar is 20 μm.

4.4 Western Blot

The same blot was probed with two different antibodies. First with m-α-GFP and later with rab-α-UL47. With the GFP antibody, a moderate signal at the height of 32 kDa was detected exclusively in the lysates of the positive control EGFP-C1. The UL47 antibody revealed a strong signal in the range of the expected size (37 kDa) in samples of LMH cells transfected with an expression plasmid for mNG-UL47_60-155. Furthermore, two faint bands at around 30-32 kDa appeared for the samples of LMH cells transfected with an expression plasmid for mNG-UL47_1-75 as well as for mNG-UL47_60-155 (Fig. 17).

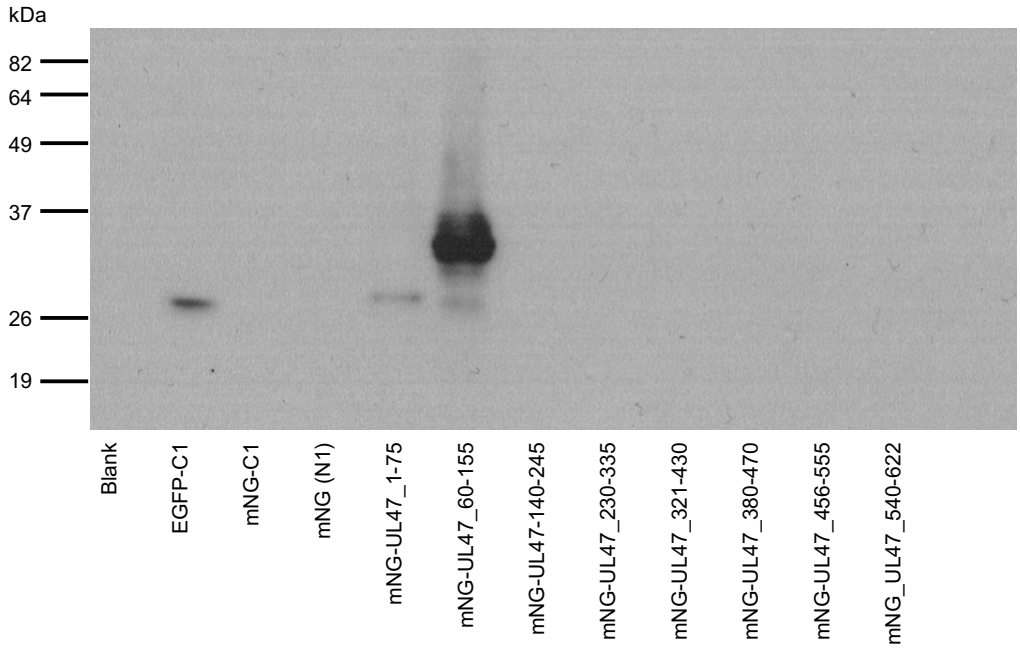

FIG. 17. Western blot of lysates of transfected 239T cells.
The blot was probed with with an GFP- and with an UL47- antibody.

4.5 Analysis of ILT reporter viruses

Viral particles detected by the gJ-antibody should get detected in the red fluorescence channel. Those particles with incorporated mNG-UL47 fusion proteins should be detected in the green fluorescence channel. Co-localization should appear as yellow spots after merging both images (Fig. 18, Table 21).

Transgene	mNG-UL47 (green)	ILT particles (red)	Co-localization
-	-	+++	-
mNG	-/+	++/+++	-
mNG-UL47_ 60-155	+	++	-
mNG-UL47_ 140-245	-	++	-
mNG-UL47_ 230-335	-	+/++	-
mNG-UL47_ 321-430	+	++	-
mNG-UL47_ 380-470	+	++	-
mNG-UL47_ 456-555	-/+	++	-
mNG-UL47_ 540-622	+	++	-

TABLE 21. Analysis of ILT reporter viruses.
The amount of fluorescent spots subjectively rated with following scores: negative: -, low: +, moderate: ++, high: +++

Neon green	ILTV particle stain (gJ)	Merged images
LMH cells		
	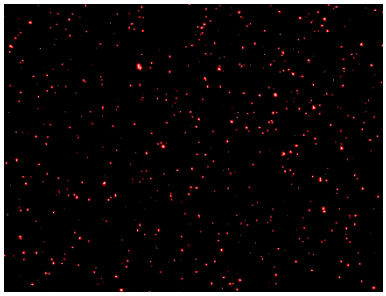	
construct **pL-mNG**		
	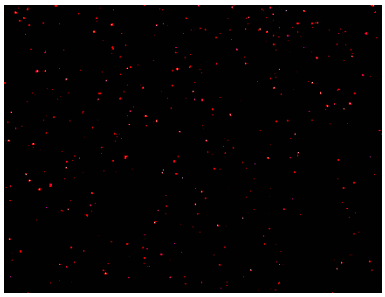	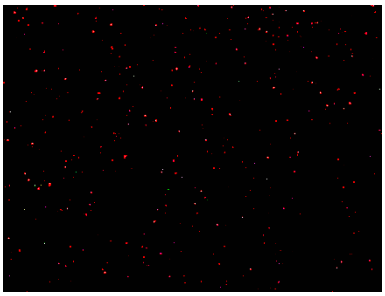
construct **pL-mNG-UL47_60-155**		
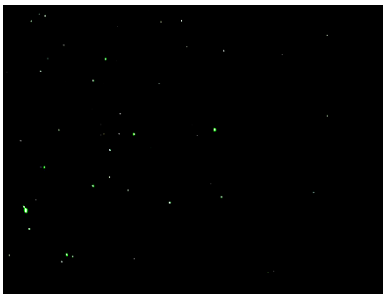	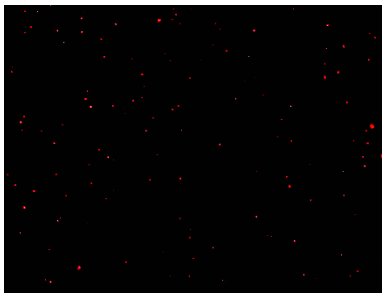	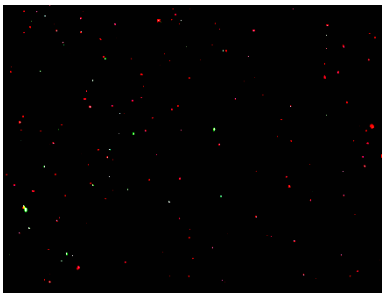
construct **pL-mNG-UL47_140-245**		
	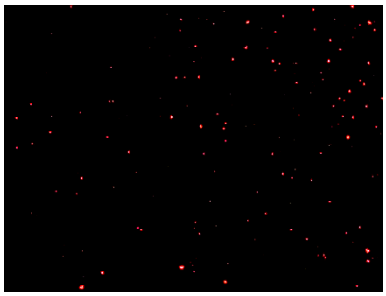	
construct **pL-mNG-UL47_230-335**		
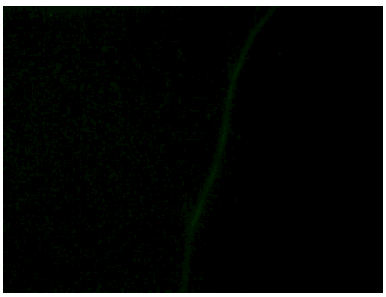	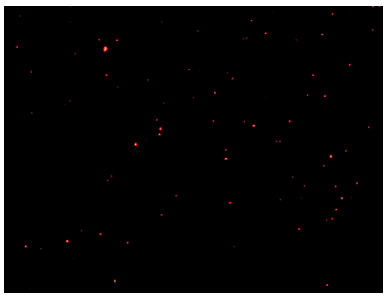	

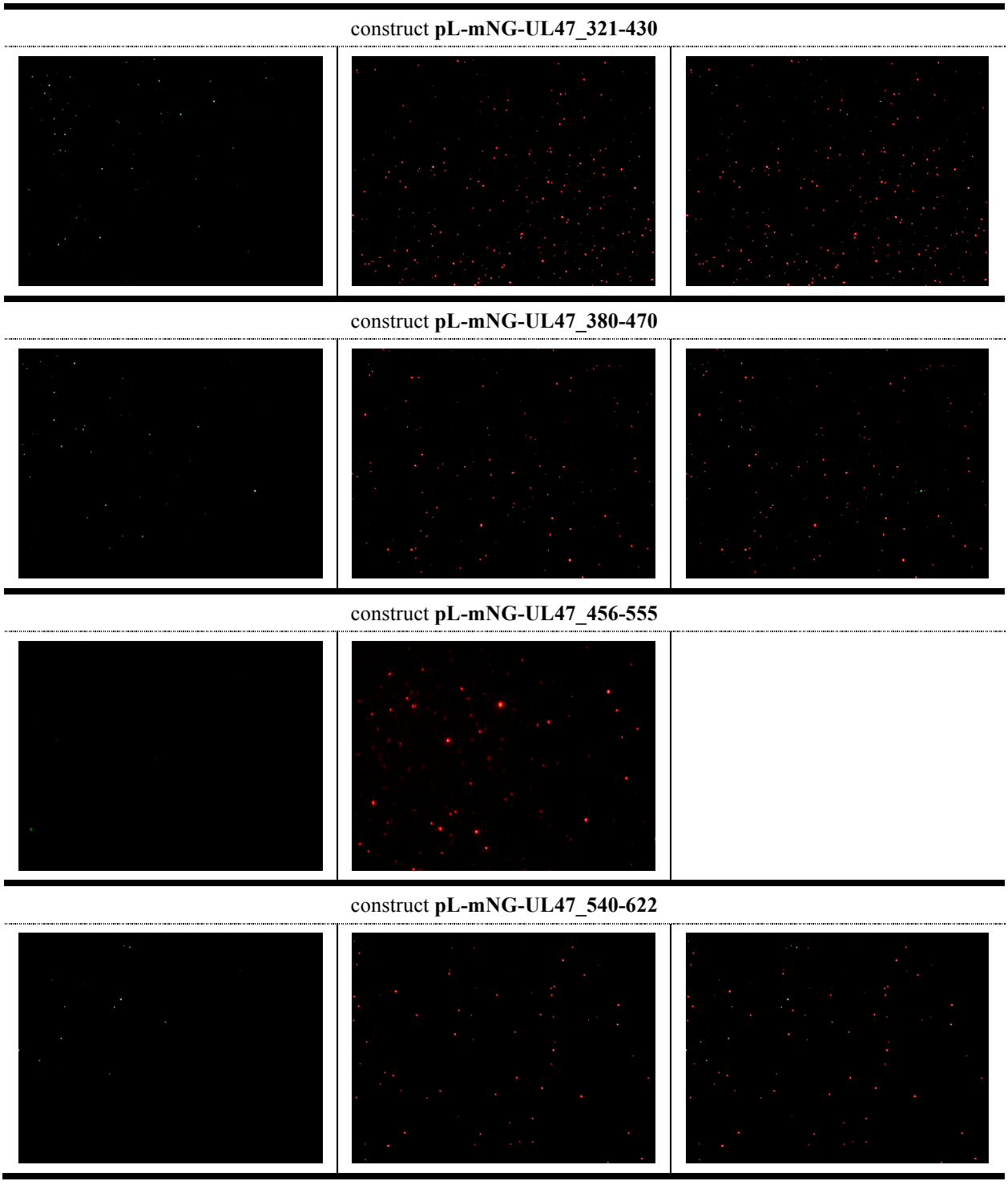

FIG. 18. ILT reporter viruses generated in mNG-UL47 expressing LMH cells.
left: green – mNG or mNG-UL47 fusion proteins, middle: red – gJ antibody stain for detection of ILTV, right: merge. 100x magnification.

5. Discussion

ILT is a worldwide distributed disease with an immense economical impact. Nowadays, still no effective vaccine, which delivers sufficient protection without leading to latent infection nor intermittent virus shedding, is developed. In addition, treatment of the disease is impossible. Thus, it is crucial to gain more insight into the virus life cycle. Reporter viruses serve as useful tools for studying virus-host interactions. With fluorescent-labelled viruses even real-time monitoring of several infection steps is possible. Therefore, the generation of ILT reporter viruses was anticipated.

The assumption of a potential packaging signal at the C-terminal end of the UL47 gene of ILTV is based on the recent work of Schlegel and Blaho 2009 and alignment of HSV-1 VP22 and ILTV UL47. This led to the generation of different mNG-UL47 fusion proteins to enable incorporation of mNG into virus particles. If the initially predicted C-terminal part of UL47 would not be responsible for protein packaging, another part of the ILTV UL47 gene might enable the incorporation. Fragmentation of the UL47 gene was required, since the entire UL47 gene was to large to be successfully fused to mNG and inserted into the expression vector.

5.1 Cloning of mNG-UL47 fusion protein transfer vectors

The amplification and fusion of the respective DNA fragments was successful as shown by agarose gel electrophoresis. Unclear bands or multiple signals resulting from non-specific amplifications were eliminated by adjusting the cycler program by a modification of the annealing temperature by 2°C. The weak bands around 300 – 400 bp detected after PCR 2 are remaining input DNA. Since the correct bands were excised from the gel, these additional bands had no impact on the following cloning reactions. Finally, PCR products of all intended fusion fragments have been produced.

Upon ligation of the mNG-UL47 fusion fragments into the expression vector pL-EGFP-N1, the following transformation was performed in *E. coli* TOP 10 F' and *E. coli* XL-10 gold. The reason for the use of two *Escherichia coli* strains was the low efficiency of the transformation of pL-mNG-N1 and pL-mNG-UL47_610-622 in the first two approaches using *E. coli* TOP 10 F' (data not shown). Transformation of pL-mNG-UL47_140-245, pL-mNG-UL47_230-335, pL-mNG-UL47_321-430, pL-mNG-UL47_380-470, pL-mNG-UL47_456-555 and pL-mNG-UL47_540-622 into *E. coli* TOP 10 F' resulted in properly grown colonies. The transformation of pL-mNG-N1, pL-mNG-UL47_610-622, pL-mNG-UL47_1-75, and mNG-UL47_60-155 into *E. coli* XL-10 gold resulted in the growth of an appropriate amount of colonies to be picked for further plasmid preparation, control restriction analysis and subsequent sequencing. *E. coli* XL-10 gold support the amplification of large plasmids which might explain the better performance of some of the transformations compared to the previous approach in *E. coli* TOP 10 F'.

After control restriction analysis, samples which showed the expected band pattern were sequenced. Eight out of nine constructs contained the correct amino acid sequences. Cloning of pL-mNG-UL47_610-622 was not successful. One explanation could be an incorrect primer. The used primers also encoded for restriction sites that were used for cloning. In rare events, point mutations can occur during primer synthesis. This could explain the unsuccessful insertion into the expression vector.

5.2 Transfection of 293T cells and generation of retroviral vectors

For the generation of retroviral vectors, 293T cells were transfected with a packaging construct, an envelope construct and the newly generated mNG-UL47 fusion fragment transfer vectors. The transfection efficiency could easily be monitored by the fluorescence of the mNG. Three constructs (pL-mNG-UL47_1-75, pL-mNG-UL47_140-245, and pL-mNG-UL47_456-555) showed very few and/or weak fluorescence. Thus, the transfection was repeated with twice the amount of plasmid, which could improve the result slightly. The reasons for these heterogenous results are difficult to figure out. Transfection experiments were proceeded in parallel and positive and negative controls showed the expected results. Major errors on the part of utilized instruments and reagents or on the part of technical aspects as preparation of 293T cells, can thereby be excluded. 293T cells are suitable and designated as highly transfectable cell lines [44]. The consideration of the optimal density of the cells before transfection, appropriate cell culture medium and cell cultivation affirm a careful and precise workflow. No contamination of transfected cells, especially with *Mycoplasma* sp. which would alter the cell morphology, could be detected at any time of the experiments. Another conceivable reason for the partially poor transfection efficiency could be due to degradation of the plasmid DNA. Therefore, control restriction analysis was performed and resulted in distinct bands as described in the previous chapter. For degraded DNA a smear would have been expected. Furthermore, only plasmids with the correct mNG-UL47 sequence were used. Since only the inserted mNG-UL47 region was sequenced, mutations in other parts of the plasmid, e.g. the promoter region, that might have occurred during the cloning process, remain possible. But the most likely reason for these results is an influence of the particular fused UL47 fragment on folding and/or localization of mNG which might have a negative effect on the fluorescence.

5.3 Transduction of LMH cells and generation of stable cell lines

Analysis of the negative control (native LMH cells) revealed a dim, blurry fluorescence due to autofluorescence. In the positive control (LMH cells transduced with the mNG transfer vector) bright fluorescent nuclei were detected but also some weaker fluorescence was observed in the cytosol. mNG-UL47_60-155 and mNG-UL47_230-335 appeared equally distributed within the nucleus and cytoplasm. mNG-UL47_540-622 showed a pronounced signal in the nuclei similar to mNG alone. In cells expressing mNG-UL47_140-245 bright fluorescent spots were detected in close proximity to the nucleus. This localization could resemble the Golgi apparatus. A counterstain of a Golgi marker, e.g. E1A could verify this assumption. mNG-UL47_321-430, mNG-UL47_380-470 and mNG-UL47_456-555 also showed a distinct spotted fluorescence pattern but in contrast to mNG-UL47_140-245 it was more dispersed over the cytosol. This localization probably corresponds to cellular vesicles like endo- and exosomes, lysosomes or peroxisomes [45]. Again, a specific antibody stain of the particular organelles would be needed for an in depth analysis of the exact localization.

ILTV UL47 was already shown to be localized within the cell nuclei as well as within the cytoplasm of infected chicken embryo kidney (CEK) cells [36]. This corresponds to the the fluorescent pattern observed for mNG-UL47_60-155 and mNG-UL47_230-335 and partially also for mNG-UL47_540-622, even though we used LMH cells. Furthermore, it was shown that the intracellular localization of a HSV-1 protein differs, dependent on the fused fluorescent protein [46]. In the presented work, the fused protein fragments influence the subcellular localization of the fluorescent protein. Thus, the UL47 fragments fused to mNG might contain motives that direct or retain the fusion protein to or in particular cell compartments.

It was striking that the total amount of fluorescent cells was rather low. Especially, since the cells were selected for their antibiotic resistance which was transferred on the same construct as the mNG-UL47 fusion fragments. However, both genes are expressed under the control of different promoters. The antibiotic resistance is driven by the promoter of the Moloney murine leukemia virus whereas the expression of the mNG-UL47 fusion fragments is under the control of the cytomegalovirus promoter. It could be, that there is a CMV promoter specific silencing mechanism in LMH cells which leads to the downregulation of mNG-UL47 fusion fragment expression or completely abolishes its expression. Nevertheless, a subset of cells showed clearly detectable fluorescent signals which differs in their patterns.

A certain correlation between fluorescence detected after transfection and fluorescence visualized after transduction was observed. mNG-UL47_1-75 which did not emit any fluorescence after transduction was already one of the weakest mNG-UL47 fusion fragments after transfection. mNG-UL47_140-245 which delivered a low to moderate fluorescence performance after transfection delivered consecutively weak signals after transduction. However, mNG-UL47_321-430 showed high fluorescence after transfection but very weak fluorescence after transduction with only very few cells showing a fluorescent signal in form

of very bright distinct spots. This might be a cell line specific effect, since human 293T cells were used for generating the retroviral vectors and chicken LMH cells for the transduction.

5.4 Western blot

To test the expression of the newly generated mNG-UL47 fusion fragments the fluorescence upon transfection was monitored. With this technique, it cannot be differentiated between protein size. Thus, a Western blot analysis was anticipated, since this method allows the discrimination between different sizes. All fusion proteins contain the full length mNG and therefore an antibody against mNG would have been feasible. However, so far no antibody specific for mNG is available. Since mNG shares some nucleotide (53%) as well as amino acid (33%) homology to EGFP, an antibody against GFP was tested. Unfortunately, the antibody does not recognize mNG only EGFP as seen for the control EGFP-C1. Albeit, the fusion proteins only contain parts of UL47, an antibody against this protein was utilized to detect the fusion proteins. Using this antibody mNG-UL47_60-155 could be visualized, what leads to the assumption that the epitope recognized by the UL47 antibody is encoded within the amino acids 60-155. Worth mentioning is the fact, that a second much weaker band at a lower molecular weight, occurred exclusively for mNG-UL47_60-155 and for mNG-UL47_1-75 but for non of the other fusion proteins. This makes it unlikely to be completely unspecific. Since there is an overlap of 15 amino acids between mNG-UL47_60-155 and mNG-UL47_1-75, the epitope can most likely pinpointed to this area. The weak, smaller band in the lane of mNG-UL47_60-155 might represent a cleavage product (Fig. 19).

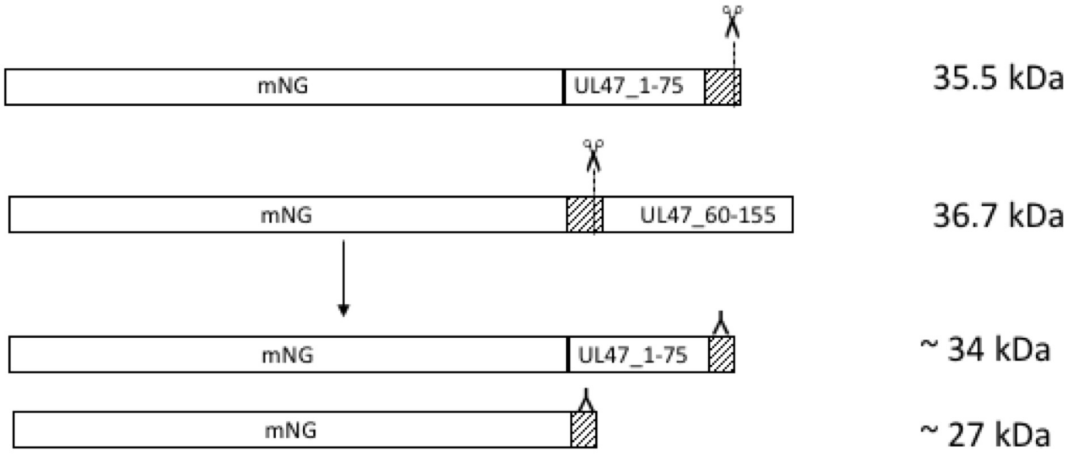

FIG. 19. Proposed antibody recognition site (Y) and protein cleavage site (✂)

It was finally not possible to detect all mNG-UL47 fusion proteins by Western blot analysis. But since all cloning products have been sequenced and fluorescence was visible, it is very likely that the anticipated constructs were generated.

5.5 Generation of ILT reporter viruses

By infecting the mNG-UL47 fusion protein expressing cell lines with a mutant ILTV lacking the UL47 gene, it was anticipated to achieve the incorporation of mNG into the newly generated ILTV particles due to the putative packaging signal of the fused UL47 fragment. This could not be shown for any of the generated fusion proteins. In some cases, (mNG-UL47_60-155, mNG-UL47_321-430, mNG-UL47_380-470, mNG-UL47_540-622) fluorescent spots were detected in the green channel. But since these spots do not co-localize with the immuno-stained ILTV particles (visible in the red channel), it is likely that these spots are artefacts and result from non-virus associated mNG protein aggregates. An often occurring issue with packaging heterologous proteins into virus capsids is the size and thus sterical hindrance. This is unlikely, since the mutant virus does not contain the wild type protein and the mNG-UL47 fusion proteins are not bigger than the original UL47 protein. A possible explanation for not detecting any incorporated mNG-UL47 fusion-protein, is the missing VPS. Maybe, in case of ILTV UL47, this signal is not only an amino acid sequence but a tertiary protein structure, which might involve several different domains. Another reason could be an intensity issue. Even if mNG is the brightest fluorescent protein currently available, the packaged amount might be to small to be recognized with a standard fluorescence microscope. Furthermore, the cellular localization of the protein might be important for packaging into the virus particle. Some of the observed fluorescent patterns could indicate an association of the respective protein to a particular cellular organelle, which might prevent packaging. Another reason for the not succeeded incorporation of the mNG-UL47 fusion proteins could be the phosphorylation status of the protein. For several HSV-1 tegument proteins it was shown, that only underphosphorylated versions are incorporated into virus particles [47], [48], [49]. Besides a particular packaging sequence and the phosphorylation status the interaction with other viral proteins might be needed for successful incorporation into virus particles as it was also shown for ICP0 another HSV-1 protein [50].

5.6 Conclusions

The aim of this study was the generation of ILT reporter viruses with incorporated mNeonGreen-UL47 fusion proteins. Cloning of the various mNG-UL47 fusion fragments, transfection of 293T cells and further transduction of LMH cells was successfully implemented in at least seven out of initially nine samples. The final goal of generating ILT reporter viruses was not succeeded. The assumed virion packaging signal, a motif of six consecutive amino acids which is similar to the one found in VP22 of HSV-1, could not be proven to exist or function in ILTV UL47.

6. References

[1] G. J. Crawshaw and B. R. Boycott, 'Infectious Laryngotracheitis in Peafowl and Pheasants', *Avian Dis.*, vol. 26, no. 2, pp. 397–401, 1982.

[2] N. C. Kirkpatrick, A. Mahmoudian, C. A. Colson, J. M. Devlin, and A. H. Noormohammadi, 'Relationship between mortality, clinical signs and tracheal pathology in infectious laryngotracheitis', *Avian Pathol.*, vol. 35, no. 6, pp. 449–453, 2006.

[3] J. R. Beach, 'Infectious bronchitis of fowls', *J. Am. Vet. Med. Assoc.*, vol. 68, pp. 570–580, 1926.

[4] F. T. W. Jordan, 'A Review of the Literature on Infectious Laryngotracheitis (ILT)', *Avian Dis.*, vol. 10, no. 1, pp. 1–26, 1966.

[5] D. E. Swayne, J. R. Glisson, L. R. McDougald, L. K. Nolan, D. L. Suarez, and V. L. Nair, *Diseases of Poultry*. Wiley, 2013.

[6] R. A. Williams, M. Bennett, J. M. Bradbury, R. M. Gaskell, R. C. Jones, and F. T. Jordan, 'Demonstration of sites of latency of infectious laryngotracheitis virus using the polymerase chain reaction', *J. Gen. Virol.*, vol. 73, pp. 2415–2420, 1992.

[7] C. S. Hughes, R. M. Gaskell, R. C. Jones, J. M. Bradbury, and F. T. Jordan, 'Effects of certain stress factors on the re-excretion of infections laryngotracheitis virus from latently infected carrier birds', *Res. Vet. Sci.*, vol. 46, pp. 274–276, 1989.

[8] S. B. Hitchner, J. Fabricant, and T. J. Bagust, 'A Fluorescent-Antibody Study of the Pathogenesis of Infectious Laryngotracheitis', *Avian Dis.*, vol. 21, no. 2, pp. 185–194, 1976.

[9] J. S. Guy, H. J. Barnes, and L. Smith, 'Increased Virulence of Modified-Live Infectious Laryngotracheitis Vaccine Virus Following Bird-to-Bird Passage', *Avian Dis.*, vol. 35, no. 2, pp. 348–355, 1991.

[10] J. S. Guy, H. J. Barnes, L. M. Morgan, N. Carolina, F. Isolates, J. S. Guy, A. H. J. Barnes, and L. M. Morgana, 'Virulence of Infectious Laryngotracheitis Viruses : Comparison of Modified-Live Vaccine Viruses and North Carolina Field Isolates', *Avian Dis.*, vol. 34, no. 1, pp. 106–113, 1990.

[11] T. J. Bagust, ‘Laryngotracheitis (Gallid-1) Herpesvirus Infection in the Chicken 4 . Latency Establishment by Wild and Vaccine Strains of ILT Virus’, *Avian Pathol.*, vol. 15, pp. 581–595, 1986.

[12] B. Müller, J. Daecke, O. T. Fackler, T. Dittmar, H. Zentgraf, H.-G. Kräusslich, B. Mu, and M. T. Dittmar, ‘Construction and Characterization of a Fluorescently Labeled Infectious Human Immunodeficiency Virus Type 1 Derivative’, *J. Virol.*, vol. 78, no. 19, pp. 10803–10813, 2004.

[13] J. Jose, J. Tang, A. B. Taylor, T. S. Baker, and R. J. Kuhn, ‘Fluorescent Protein-Tagged Sindbis Virus E2 Glycoprotein Allows Single Particle Analysis of Virus Budding from Live Cells’, *Viruses*, vol. 7, pp. 6182–6199, 2015.

[14] D. R. Thureen and C. L. Keeler, ‘Psittacid Herpesvirus 1 and Infectious Laryngotracheitis Virus: Comparative Genome Sequence Analysis of Two Avian Alphaherpesviruses’, *J. Virol.*, vol. 80, no. 16, pp. 7863–7872, Aug. 2006.

[15] A. J. Davison, ‘Herpesvirus systematics’, *Vet. Microbiol.*, vol. 143, pp. 52–69, 2010.

[16] M. A. Johnson and S. G. Tyack, ‘Molecular evolution of infectious laryngotracheitis virus (ILTV; gallid herpesvirus 1): An ancient example of the Alphaherpesviridae?’, in *Veterinary Microbiology*, 1995, vol. 46, pp. 221–231.

[17] D. J. Mcgeoch, A. Dolan, and A. C. Ralph, ‘Toward a Comprehensive Phylogeny for Mammalian and Avian Herpesviruses’, *J. Virol.*, vol. 74, no. 22, pp. 10401–10406, 2000.

[18] W. Fuchs, D. Wiesner, J. Veits, J. P. Teifke, and T. C. Mettenleiter, ‘In Vitro and In Vivo Relevance of Infectious Laryngotracheitis Virus gJ Proteins That Are Expressed from Spliced and Nonspliced mRNAs’, *J. Virol.*, vol. 79, no. 2, pp. 705–716, 2005.

[19] D. J. McGeoch, M. A. Dalrymple, A. J. Davison, A. Dolan, M. C. Frame, D. McNab, L. J. Perry, J. E. Scott, and P. Taylor, ‘The Complete DNA Sequence of the Long Unique Region in the Genome of Herpes Simplx Virus Type 1’, *J. Gen. Virol.*, vol. 69, pp. 1531–1574, 1988.

[20] M. A. Johnson, C. T. Prideaux, K. Kongsuwan, M. Sheppard, and K. J. Fahey, ‘Gallid herpesvirus 1 (infectious laryngotracheitis virus): cloning and physical maps of the SA-2 strain’, *Arch. Virol.*, vol. 119, pp. 181–198, 1991.

[21] D. A. Leib, J. M. Bradbury, C. A. Hart, and K. McCarthy, ‘Genome Isomerism in Two Alphaherpesviruses: Herpesvirus saimiri-1 (Herpesvirus tamarinus) and Avian Infectious Laryngotracheitis Virus’, *Arch. Virol.*, vol. 93, pp. 287–294, 1987.

[22] K. Ziemann, T. C. Mettenleiter, and W. Fuchs, ‘Gene Arrangement within the Unique Long Genome Region of Infectious Laryngotracheitis Virus Is Distinct from That of Other Alphaherpesviruses’, *J. Virol.*, vol. 72, no. 1, pp. 847–852, 1998.

[23] K. Ziemann, T. C. Mettenleiter, and W. Fuchs, ‘Infectious Laryngotracheitis Herpesvirus Expresses a Related Pair of Unique Nuclear Proteins Which Are Encoded by Split Genes Located at the Right End of the UL Genome Region’, *J. Virol.*, vol. 72, no. 8, pp. 6867–6874, 1998.

[24] D. Helferich, J. Veits, J. P. Teifke, T. C. Mettenleiter, and W. Fuchs, ‘The UL47 gene of avian infectious laryngotracheitis virus is not essential for in vitro replication but is relevant for virulence in chickens’, *J. Gen. Virol.*, vol. 88, pp. 732–742, Mar. 2007.

[25] M. A. Wild, S. Cook, and M. Cochran, ‘A Genomic Map of Infectious Laryngotracheitis Virus and the Sequence and Organization of Genes Present in the Unique Short and Flanking Regions’, *Virus Genes*, vol. 12, no. 2, pp. 107–116, 1996.

[26] F. Dorange, B. K. Tischer, and N. Osterrieder, ‘Characterization of Marek’s Disease Virus Serotype 1 (MDV-1) Deletion Mutants That Lack UL46 to UL49 Genes: MDV-1 UL49, Encoding VP22, Is Indispensable for Virus Growth’, *J. Virol.*, vol. 76, no. 4, pp. 1959–1970, 2002.

[27] M. Kopp, B. G. Klupp, H. Granzow, W. Fuchs, and T. C. Mettenleiter, ‘Identification and Characterization of the Pseudorabies Virus Tegument Proteins UL46 and UL47: Role for UL47 in Virion Morphogenesis in the Cytoplasm’, *J. Virol.*, vol. 76, no. 17, pp. 8820–8833, 2002.

[28] Y. Zhang, D. a Sirko, and J. L. McKnight, ‘Role of Herpes Simplex Virus Type 1 UL46 and UL47 in alpha TIF-Mediated Transcriptional Induction: Characterization of Three Viral Deletion Mutants’, *J. Virol.*, vol. 65, no. 2, pp. 829–841, Feb. 1991.

[29] R. Klopfleisch, B. G. Klupp, W. Fuchs, M. Kopp, J. P. Teifke, and T. C. Mettenleiter, ‘Influence of Pseudorabies Virus Proteins on Neuroinvasion and Neurovirulence in Mice’, *J. Virol.*, vol. 80, no. 11, pp. 5571–5576, 2006.

[30] E. F. M. Schlegel and J. A. Blaho, ‘A conserved carboxy-terminal domain in the major tegument structural protein VP22 facilitates virion packaging of a chimeric protein during productive herpes simplex virus 1 infection’, *Virology*, vol. 387, no. 2, pp. 449–458, May 2009.

[31] N. C. Shaner, G. G. Lambert, A. Chammas, Y. Ni, P. J. Cranfill, M. A. Baird, B. R. Sell, J. R. Allen, R. N. Day, M. Israelsson, M. W. Davidson, and J. Wang, ‘A bright monomeric green fluorescent protein derived from Branchiostoma lanceolatum’, *Nat. Am.*, vol. 10, no. 5, pp. 407–409, 2013.

[32] T. Kawaguchi, K. Nomura, Y. Hirayama, and T. Kitagawa, ‘Establishment and Characterization of a Chicken Hepatocellular Carcinoma Cell Line, LMH1’, *Cancer Res.*, vol. 47, pp. 4460–4464, 1987.

[33] W. M. Schnitzlein, J. Radzevicius, and D. N. Tripathy, ‘Propagation of Infectious Laryngotracheitis Virus in an Avian Liver Cell Line’, *Avian Dis.*, vol. 38, pp. 211–217, 1994.

[34] E. Scholz, E. Welniak, T. Nyholm, and P. Guo, ‘An avian hepatoma cell line for the cultivation of infectious laryngotracheitis virus and for the expression of foreign genes with a mammalian promotor’, *J. Virol. Methods*, vol. 43, pp. 273–286, 1993.

[35] Y. Soneoka, P. M. Cannon, E. E. Ramsdale, J. C. Griffiths, G. Romano, S. M. Kingsman, and A. J. Kingsman, ‘A transient three-plasmid expression system for the production of high titer retroviral vectors’, *Nucleic Acids Res.*, vol. 23, no. 4, pp. 628–633, 1995.

[36] D. Helferich, J. Veits, T. C. Mettenleiter, and W. Fuchs, ‘Identification of transcripts and protein products of the UL31, UL37, UL46, UL47, UL48, UL49 and US4 gene homologues of avian infectious laryngotracheitis virus’, *J. Gen. Virol.*, vol. 88, pp. 719–731, Mar. 2007.

[37] S. Andreadis and B. O. Palsson, ‘Coupled Effects of Polybrene and Calf Serum on the of Efficiency of Retroviral Transduction and the Stability Retroviral Vectors’, *Hum. Gene Ther.*, vol. 8, pp. 285–291, 1997.

[38] H. E. Davis, J. R. Morgan, and M. L. Yarmush, ‘Polybrene increases retrovirus gene transfer efficiency by enhancing receptor-independent virus adsorption on target cell membranes’, *Biophys. Chem.*, vol. 97, pp. 159–172, Jun. 2002.

[39] G. M. Springett, R. C. Moen, S. Anderson, R. M. Blaese, and W. F. Anderson, 'Infection Efficiency of T Lymphocytes with Amphotropic Retroviral Vectors Is Cell Cycle Dependent', *J. Virol.*, vol. 63, no. 9, pp. 3865–3869, 1989.

[40] D. G. Miller, M. A. Adam, and A. D. Miller, 'Gene Transfer by Retrovirus Vectors Occurs Only in Cells That Are Actively Replicating at the Time of Infection', *Mol. Cell. Biol.*, vol. 10, no. 8, pp. 4239–4242, 1990.

[41] K. Toyoshima and P. K. Vogt, 'Enhancement and Inhibition of Avian Sarcoma Viruses by Polycations and Polyanions', *Virology*, vol. 38, pp. 414–426, 1969.

[42] J. Davies and A. Jimenez, 'A New Selective Agent for Eukaryotic Cloning Vectors', *Am. J. Trop. Med. Hyg.*, vol. 29, no. 5, pp. 1089–1092, 1980.

[43] M. M. Bradford, 'A Rapid and Sensitive Method for the Quantitation of Microgram Quantities of Protein Utilizing the Principle of Protein-Dye Binding', *Anal. Biochem.*, vol. 72, pp. 248–254, 1976.

[44] W. S. Pear, G. P. Nolan, M. L. Scott, and D. Baltimore, 'Production of high-titer helper-free retroviruses by transient transfection', *Cell Biol.*, vol. 90, pp. 8392–8396, 1993.

[45] C. Stadler, E. Rexhepaj, V. R. Singan, R. F. Murphy, R. Pepperkok, M. Uhlén, J. C. Simpson, and E. Lundberg, 'Immunofluorescence and fluorescent-protein tagging show high correlation for protein localization in mammalian cells', *Nat. Am.*, vol. 10, no. 4, pp. 315–323, 2013.

[46] A. Söling, A. Simm, and N. G. Rainov, 'Intracellular localization of Herpes simplex virus type 1 thymidine kinase fused to different fluorescent proteins depends on choice of fluorescent tag', *FEBS Lett.*, vol. 527, pp. 153–158, 2002.

[47] D. M. Meredith, J. A. Lindsay, W. Halliburton, and G. R. Whittaker, 'Post-translational modification of the tegument proteins (VP13 and VP14) of herpes simplex virus type 1 by glycosylation and phosphorylation', *J. Gen. Virol.*, vol. 72, pp. 2771–2775, 1991.

[48] G. Elliott, D. O. Reilly, and P. O. Hare, 'Phosphorylation of the Herpes Simplex Virus Type 1 Tegument Protein VP22', *Virology*, vol. 226, no. 0638, pp. 140–145, 1996.

[49] J. S. Loomis, R. J. Courtney, and J. W. Wills, ‘Packaging Determinants in the UL11 Tegument Protein of Herpes Simplex Virus Type 1’, *J. Virol.*, vol. 80, no. 21, pp. 10534–10541, 2006.

[50] K. Maringer and G. Elliott, ‘Recruitment of Herpes Simplex Virus Type 1 Immediate-Early Protein ICP0 to the Virus Particle’, *J. Virol.*, vol. 84, no. 9, pp. 4682–4696, 2010.

7. Figures and tables

7.1 Figures

7.2 Tables

8. Appendix

8.1 Index of abbreviations

°C	degree Celsius
293T	Human embryonic kidney (cell line)
bp	base pairs
c-terminal	carboxy-terminal
CEK	chicken embryo kidney (cell line)
cm	centimetre
cm^2	square centimetre
CMV	cytomegalovirus
cs	coverslip
DAPI	4',6-diamidino-2-phenylindole
dATP	deoxyadenosine triphosphate
DC	direct current
ddH_2O	double-distilled water
DIC	differential interference contrast
DIVA	Differentiating Infected from Vaccinated Animals
DMEM	Dulbecco's Modified Eagle Medium
DNA	deoxyribonucleic acid
dNTP	deoxynucleoside triphosphate
E. coli	*Escherichia coli*
E1A	adenoviral early region 1A
ECL	enhanced chemiluminescence
EDTA	ethylenediaminetetraacetic acid
EGFP	enhanced green fluorescent protein
EtBr	ethidium bromide
FBS	fetal bovine serum
g	g-force / relative centrifugal force

G418	Geneticin
GaHV-1	gallid herpesvirus 1
GFP	green fluorescent protein
gJ	glycoprotein J
h	hour
HSV-1	herpes simplex virus 1
HSV-2	herpes simplex virus 2
ILT	infectious laryngotracheitis
ILTV	infectious laryngotracheitis virus
kb	kilo base pairs
kDa	kilodalton
LMH	Leghorn Male Hepatoma (cell line)
LTR	long terminal repeat
MDV-1	Marek's disease virus serotype 1
mg	milligram
min	minute
ml	millilitre
mM	millimolar
mNG	monomeric NeonGreen
Neo^R	Neomycin resistance gene
ng	nanogram
ORF	open reading frame
P/S	Penicillin-Streptomycin
PBS	phosphate buffered saline
PCR	polymerase chain reaction
PES	polyethersulfone
PFA	paraformaldehyde

PrV	pseudorabies virus
PsHV-1	psittacid herpes virus 1
qPCR	real-time polymerase chain reaction
RFP	red fluorescent protein
rpm	revolutions per minute
RT	room temperature
s	second
SN	supernatant
sp.	species
TAE	Tris-Acetat-EDTA
TBS	Tris-buffered saline
TTBS	TBS containing Tween20
UL	unique long
US	unique short
V	volt
VPS	virion packaging signal
VZV	Varicella zoster virus
wt	wild type
µg	microgram
µl	microliter
µm	micrometre

8.2 Acknowledgments

An dieser Stelle möchte ich meinen ausdrücklichen Dank an folgende Personen richten, welche mich während der Erstellung meiner Dissertationsschrift fortwährend unterstützt haben.

Mein uneingeschränkter Dank gilt Herrn Prof. Dr. med. vet. Richard Hoop, welcher mir die Möglichkeit gab, am Institut für Veterinärbakteriologie in der Abteilung für Geflügelkrankheiten einerseits meine Dissertation zu erstellen, andererseits gleichzeitig als Assistenztierärztin zu arbeiten um wertvolle klinische Erfahrungen sammeln zu können. Für seine kontinuierliche Unterstützung und Geduld, sowie für die Funktion als Referent, möchte ich mich sehr bedanken.

Ein grosses Dankeschön möchte ich auch Herrn Prof. Dr. sc. nat. Cornel Fraefel, in der Funktion als Korreferent, für die sorgfältige Prüfung meiner Dissertationsschrift aussprechen.

Für die hervorragende wissenschaftliche Betreuung, sowie die stetige Unterstützung während den Experimenten und der Niederschrift, möchte ich mich ganz herzlich bei Dr. Nina Wolfrum bedanken. Die umgehende Durchsicht, die differenzierte Überarbeitung und wertvollen Ergänzungen meines Manuskripts, sowie die stets positiven mentalen Inputs und ihre Geduld, erlaubten mir, eine sorgfältige und gewissenhafte Ausarbeitung meiner Dissertation.

Ein besonderes Dankeschön gilt auch allen noch nicht erwähnten Mitarbeiterinnen der Geflügelabteilung, insbesondere Brigitte Sigrist für ihre Hilfe und Erklärungen, sowie ihre exakte Arbeit während den Experimenten und Sarah Albini für ihre wertvolle fachliche Unterstützung bei meiner Arbeit als Assistenztierärztin. Die positive, kollegiale Arbeitsatmosphäre in der Abteilung, sowie die immerzu dargebotene Hilfe in allen Belangen, erleichterten mir meine Arbeit enorm.

Marco Möri, meinen Eltern Martina und Fredi Meier und meinen Freunden bin ich für die ermunternden und im positiven Sinne antreibenden Worte von ganzem Herzen dankbar. Ihre nicht-fachliche, mentale, immer wohlgesinnte Unterstützung, die Geduld und die Rücksichtnahme, waren für mich von unschätzbarem Wert.

9. Curriculum Vitae

Vorname Name	Simone Martina Meier
Geburtsdatum	04. Oktober 1985
Geburtsort	Winterthur, ZH
Nationalität	Schweiz
Heimatort	Bachenbülach, ZH
08/1992 – 07/1998	Primarschule, Ettenhausen, Schweiz
08/1998 – 07/2000	Sekundarschule, Aadorf, Schweiz
08/2000 – 06/2004	Kantonsschule, Frauenfeld, Schweiz
25. Juni 2004	Eidgenössische Matura, Kantonsschule, Frauenfeld, Schweiz
10/2005 – 10/2010	Veterinärmedizin, Universität Zürich, Zürich, Schweiz
14. Oktober 2010	Diplom Tierärztin, Universität Zürich, Zürich, Schweiz
02/2011 – 03/2011	Praktikum in Non-Profit-Kleintierpraxis für Tiere der Einwohner von Soweto, Roodepoort, Johannesburg, Südafrika
04/2011 – 05/2011	Assistentin, ACR Kleintierpraxis, Winterthur, Schweiz
11/2012 – 03/2013	Assistentin, Animaldoc, Weinfelden, Schweiz
11/2013 – 04/2017	Anfertigung der Dissertation unter Leitung von Prof. Dr. med. vet. Richard Hoop am Institut für Veterinärbakteriologie in der Abteilung für Geflügelkrankheiten, Vetsuisse-Fakultät Universität Zürich